Bioorganic Chemistry 91 (2019) 103169

Contents lists available at ScienceDirect

Bioorganic Chemistry

journal homepage: www.elsevier.com/locate/bioorg

Review article

FtsZ inhibitors as a new genera of antibacterial agents

Swayansiddha Tripathy*, Susanta Kumar Sahu

University Department of Pharmaceutical Sciences, Utkal University, Vani Vihar, Bhubaneswar 751004, Odisha, India

ARTICLE INFO

Keywords:
FtsZ
Z-ring
Protofilament
Cytokinesis
GTPase
FtsZ inhibitors

ABSTRACT

The continuous emergence and rapid spread of a multidrug-resistant strain of bacterial pathogens have demanded the discovery and development of new antibacterial agents. A highly conserved prokaryotic cell division protein FtsZ is considered as a promising target by inhibiting bacterial cytokinesis. Inhibition of FtsZ assembly restrains the cell-division complex known as divisome, which results in filamentation, leading to lysis of the cell. This review focuses on details relating to the structure, function, and influence of FtsZ in bacterial cytokinesis. It also summarizes on the recent perspective of the known natural and synthetic inhibitors directly acting on FtsZ protein, with prominent antibacterial activities. A series of benzamides, trisubstituted benzimidazoles, isoquinolene, guanine nucleotides, zantrins, carbonylpyridine, 4 and 5-Substituted 1-phenyl naphthalenes, sulindac, vanillin analogues were studied here and recognized as FtsZ inhibitors that act either by disturbing FtsZ polymerization and/or GTPase activity. Doxorubicin, from a U.S. FDA, approved drug library displayed strong interaction with FtsZ. Several of the molecules discussed, include the prodrugs of benzamide based compound PC190723 (TXA-709 and TXA707). These molecules have exhibited the most prominent antibacterial activity against several strains of *Staphylococcus aureus* with minimal toxicity and good pharmacokinetics properties. The evidence of research reports and patent documentations on FtsZ protein has disclosed distinct support in the field of antibacterial drug discovery. The pressing need and interest shall facilitate the discovery of novel clinical molecules targeting FtsZ in the upcoming days.

1. Introduction

Cell division is a crucial event in the life of every organism. Eukaryotic cells divide by processes known as “mitosis” or “meiosis”, while archaeal and bacterial cells usually divide through a process called “binary fission”, in which a septum is placed at a position called the division site in a cell to separate it into two new daughter cells. Both of the newly formed daughter cells contain a copy of the chromosome and other necessary components required for viability and functionality. Bacterial infection has become an alarming health hazard in the developing world. Nowadays many bacterial strains have become resistant to existing antibiotics making the treatment ineffective. Therefore, there is an urgent need for the development of new antibacterial agents with novel mechanisms of action that can solve the growing resistance problem.

Filamentous temperature-sensitive protein Z (FtsZ), a tubulin homolog, is the most abundant and highly conserved cell division protein across almost all bacteria. FtsZ is a prokaryotic homolog of the eukaryotic cytoskeletal protein tubulin. It plays a virtual role in prokaryotic cell division. The process of bacterial cell division is a novel and attractive target for new antibacterial drug discovery. In the 1960s, genes designated “Fts” (filament-forming temperature-sensitive genes, *fts*), were identified by mutational analysis in *Escherichia coli.* The gene products of the Fts-genes are known to be involved in septum formation, Z ring formation and the initiation of cell division [1].

Genetic studies have indicated the existence of genes regulating normal cell growth and division process. These genes were further analyzed using temperature-sensitive mutants. Temperature-sensitive (TS) mutations are powerful tools for regulating gene function. The temperature-sensitive mutations are functional at low (permissive 86 °F/30 °C) temperatures, yet non-functional at high (nonpermissive, 104–108 °F/40–42 °C) temperatures, and thus a rise in temperature quickly alter protein function [2]. Mostly the bacterial cell resume to

Abbreviations: Bs, *Bacillus subtilis*; CAMH, cation-adjusted Mueller-Hinton broth; CFU, colony forming unit; DAPI, 4′,6-diamidino-2-phenylindole; *E. coli*, *Escherichia coli*; FtsZ, filamentous temperature sensitive protein Z; GTP, guanosine 5′-triphosphate; GDP, guanosine 5′-diphosphate; IC50, half maximal inhibitory concentration; LRSA, linezolid-resistant *Staphylococcus aureus*; MBC, minimal bactericidal concentration; MIC, minimum inhibitory concentration; MRSA, methicillin-resistant *Staphylococcus aureus*; MSSA, methicillin-sensitive *Staphylococcus aureus*; Mtb, mycobacterium tuberculosis; OTBA, 3-{5-[4-oxo-2-thioxo-3-(3-trifluoromethylphenyl) thiazolidin-5-ylidenemethyl]furan-2-yl} benzoic acid; VISA, vancomycin-intermediate *Staphylococcus aureus*; VRSA, vancomycin-resistant *Staphylococcus aureus*

* Corresponding author.
E-mail address: swayansiddha@gmail.com (S. Tripathy).

https://doi.org/10.1016/j.bioorg.2019.103169
Received 14 December 2018; Received in revised form 28 July 2019; Accepted 29 July 2019
Available online 30 July 2019

grow without cell division at the restrictive temperature. The elongation of cells without cell division are called filaments that contain multiple chromosomes. The FtsZ-ring was assembled in all cells very early in the cell cycle and that at non-permissive temperatures, at which long filamentous bacteria are formed, multiple Z-rings were localized at precise intervals along with the cell.

FtsZ is considered as an appealing target for new antibacterial drug discovery for several key reasons. First, it is an essential protein for bacterial viability [3–5]. Second, FtsZ acts as a potentially broad-spectrum antibacterial agent, capable of fighting polymicrobial infection and when the etiology of the infectious agent is unknown. The FtsZ protein is highly conserved in prokaryotes, and have been identified in most bacteria. The genomic sequence data and several analysis programs of more than 850 bacteria are readily available which help to identify bacterial species containing FtsZ. Genomic sequence data has disclosed that several of the disease-causing by bacteria [6] including *Escherichia coli, Staphylococcus aureus, Mycobacterium tuberculosis, Mycoplasma genitalium, Mycoplasma pneumoniae, Helicobacter pylori, Treponema pallidum, Neisseria meningitides, Rickettsia prowazeki, Campylobacter jejuni, Shigella, Salmonella,* and many other clinically relevant microorganisms possess FtsZ. Third, FtsZ is not present in higher eukaryotes, which suggests that FtsZ inhibitors should not be toxic to human cells. Finally, because cell division proteins are not targeted by any licensed antibiotics, it is anticipated that there would not be cross-resistance within existing drug-resistant bacterial populations, as it is widespread for other classes of antibiotics, such as the β-lactams.

FtsZ is believed to be the major cytoskeletal protein played a major role in bacterial cell division. In this review, we describe the role of FtsZ in bacterial cytokinesis. Furthermore, we discuss the development of different classes of inhibitors targeting FtsZ, giving special attention to their antibacterial activities, mechanisms of action, synthetic methods, and evaluate the challenges and future prospects of research in the field of antibacterial agent.

2. Structure and function of FtsZ

2.1. FtsZ structure

FtsZ shares structural and functional features of 40–50% sequence identity across most bacterial, many archaea, some chloroplasts, and few primitive mitochondria. The three- dimensional structure of some FtsZ bacteria are similar to the structure of α- and β-tubulin [7]. Tubulin is the key component of eukaryotic microtubules. Both of the protein FtsZ and tubulin are shown to play an important role in living cells like maintenance of cell shape, structure and cell division.

FtsZ exists in the bacterial cells both as monomers or higher-order polymers depending on whether it is bound to guanosine 5′-triphosphate (GTP) or guanosine 5′-diphosphate (GDP). FtsZ protein has two enzymatic domains with distinct folds like *N*-terminal is connected C-terminal domain with different extensions and a C-terminal tail. Again the enzymatic domain consists of two globular sub-domains, designated as the *N*-terminal subdomain and C-terminal subdomain, which are separated by the central core H7 helix. The *N*-terminal enzymatic domain contains a nucleotide-binding pocket, and the C-terminal subdomain includes a GTPase-activating site (Fig. 1). Moreover, the *N*-terminal enzymatic domain and the long C-terminal domain are linked together through an H5 helix [8,9]. C-terminal domain involved in the formation of the protofilament. The active site of GTPase can be found between the two monomers. The long C-terminal tail is not properly structured and acknowledge with several the accessory proteins [10,11].

The C-terminal peptide is not involved in assembly formation but is crucial for interactions with other membrane-associated cell division proteins including FtsZ inducers, FtsA, and ZipA for the stability of Z-ring. The rupture of the C-terminal peptide disrupts FtsZ function, certainly by preventing its interaction with both cell division proteins,

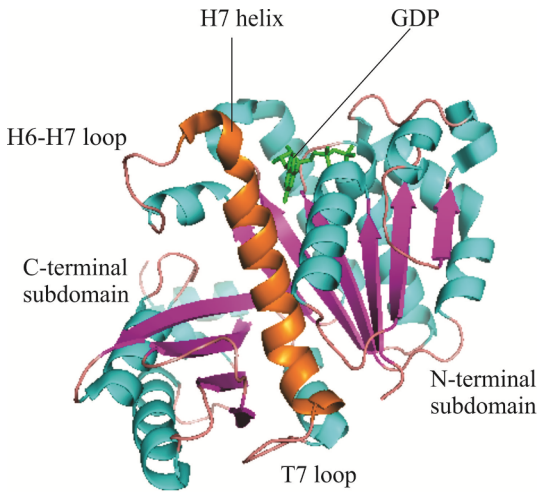

Fig. 1. Structures of FtsZ of *B. subtilis* FtsZ with GDP (PDB entry 2RHL).

FtsA, and ZipA [12]. Besides tubulin is a stable heterodimer consisting of α and β subunits whereas FtsZ subunits are identical encompass with only one form of FtsZ monomers [13]. GTPase activity of FtsZ was originally activated by the sequence representing GGGTGTG, very closely resembling the signature sequence, (G/A) GGTGSG, existing in all α, β, and γ subunit types of tubulin signature motif [14]. Concurrently, FtsZ and tubulin have a common fold, with two domains linked by α-helix [15].

Bi and Lutkenhaus suggested the first evidence that FtsZ is a cytoskeletal protein localized in a ring at the center of the cell by their immunoelectron microscopy study [16]. Another significant advance immunofluorescence images by using a FtsZ-GFP chimera allowing more precise localization of the protein. Using this approach, the ring structure was clearly observable in a three-dimensional view. It was shown that the Z-ring is assembled very early in the bacterial life cycle and the localization of the Z-ring in different species was varied. For instance, in *E. coli*, the ring was not observed at the end of cells, whereas in *B. subtilis*, small spots remained at separation sites after a new Z-ring had formed [17]. The analysis of the Z ring in E. coli using fluorescence recovery after photo bleaching (FRAP) and green fluorescent protein-labeled FtsZ (GFP) showed that the Z ring is extremely dynamic and continually remodeling itself with a half-time of 30 s [18]. Super-resolution light microscopy results suggest that the Z-ring of *E. coli* is composed of a loose bundle of FtsZ protofilaments [19,20] possibly cross-linked by several accessory divisome proteins. The lateral association of FtsZ protofilament is different from the longitudinal association of tubulin protofilament and this leads to the formation of an arc-shaped Z-ring [21].

Interestingly, *M. tuberculosis* FtsZ (*Mtb*FtsZ) has a single cysteine residue at position 155, whereas no cysteine is present in its *E. coli* or *B. subtilis* counterpart. Cysteine being a free sulfhydryl-containing amino acid plays important roles in the structure and function of various proteins. The region around cysteine residue in MtbFtsZ may play a critical role in regulating FtsZ assembly and the Z-ring formation in vivo in *M. tuberculosis*. So it indicates the possibility of using sulfhydryl-directed agents to specifically inhibit the assembly of FtsZ in *M. tuberculosis* [22].

2.2. FtsZ function

2.2.1. Role of FtsZ in bacterial cell division

Bacterial cell division is a complex process that requires accurate identification of the division site, the positioning of the division machinery, and coordinated constriction of the inner membrane and the cell wall (i.e., cytokinesis). Cytokinesis occurs in two discrete stages: the

formation of an initial, small invagination at the site of the septum, followed by the completion of cell division. FtsZ is necessary throughout both stages. The gene products of the *Fts*-genes are known to be involved in septum formation [23,24].

FtsZ is the first protein to move to the division site. This essential process is initiated with the polymerization of FtsZ into a filamentous, ring-like structure (referred to as the Z-ring) via GTP dependent polymerization. This process is initiated in the cytoplasm peripheral to the membrane and close to the division site [25–27]. With GTP, FtsZ assembles on the inner membrane at mid-cell to form a highly dynamic helical structure [28]. FtsZ can also form Z-ring encircling the cell [29]. Following the recruitment of other necessary cell division proteins to the middle of the cell, the Z-ring will contract and result in the septum formation at the mid-cell to mediate normal cell division process [30]. The Z-ring acts as a framework for the recruitment of at least twelve additional cell division proteins to form a cell-division complex called a divisome which constricts the membrane resulting septum formation at mid-cell to mediate normal cell division process. FtsZ activity is subject to the regulation of some FtsZ interacting proteins. ZapA, ZipA, and FtsA are stabilizing factors, while SulA, EzrA, and MinCD are destabilizing factors [31,32].

FtsZ initially assembles isometrically as a curved protofilament, but after reaching a certain length the protofilament ends are able to contact each other. This process of cyclization would cause the formation of additional lateral bonds, resulting in cooperativity. In accord with this model, protofilament rings, some hundreds of nanometers in diameter, have been observed by atomic force microscopy and electron microscopy [33].

The rod-shaped bacteria, such as the Gram-negative *E. coli*, produces long, filamentous cells on depletion of FtsZ due to the continued growth of cells that are no longer dividing. Cocci-shaped bacteria, Gram-positive pathogen *S. aureus*, increase in volume up to 8-fold on depletion of FtsZ. In both cases, cells are unable to divide; continued growth makes them enlarged and sensitive to changes in the physical properties of their environment, and the cells eventually lyse [34]. On a target of position, activity, and interaction of FtsZ with other division protein cause lysis of cell and may be useful in the development of new antibacterial agents.

2.2.2. Dynamic function of FtsZ

During different stages of the cell, cycle FtsZ exhibits a series of different behaviors: assembly to form the Z ring at mid-cell, maintenance of the ring through continual subunit turnover, and constriction and disassembly of the ring. The transitions between Z ring growth, maintenance, and constriction are likely to be regulated by factors that influence FtsZ's assembly dynamics. FtsZ exists in the cytoplasmic pool in the form of monomers and oligomers. Generally, there are as many as 15,000 FtsZ molecules in each *E. coli* cell, and their concentration remains constant during the entire cell cycle, but only about 30% of these participate in Z-ring formation at a given time [35,36]. Each subunit of hydrolyzed GDP-bound FtsZ can be exchanged independently with GTP-bound FtsZ in the cytoplasm. The suitable quantities of FtsZ protein in the cytoplasm eliciting nucleotide exchange with rapid equilibration in favor of GTP bound FtsZ. After a certain critical concentration, GTP-bound FtsZ is favored, polymerization begins and long-straight protofilaments begin to form. During polymerization, GTP hydrolysis is in continuous competition with protofilament growth in a process referred to 'steady-state turnover' [37]. The in vitro study suggests the possibility that GTP-bound FtsZ assembles as linear protofilaments inside the cell and then, associate into bundles to form the highly dynamic Z-ring (Fig. 2). The biochemical studies and electron microscopic analysis to show that straight and curved conformations of FtsZ protofilaments are favored by GTP and GDP, respectively, indicating that the GTP hydrolysis leads to this structural transition [38].

After bacterial cell division occurs, regulation of GTP yields distorted GDP-bound FtsZ-dominated protofilaments that revert to the monomer form. GTP hydrolysis is generally determined as the amount of phosphate released after hydrolysis, providing a measure of GTP turnover. GDP release may occur either by direct nucleotide exchange in the polymers [39,40] or via depolymerization and subsequent nucleotide exchange in the monomers. The release of Pi is the trigger for a conformational change [41] that destabilizes the polymer or leads to the straight/curved transition. These dynamics, termed 'steady-state turnover', show an alternative model for Z-ring formation and contraction. From the published data, it is pointed out that the nucleotide turnover rate can vary from 6.9 nmol mg^{-1} h^{-1} for *M. tuberculosis* to 30 mmol mg^{-1} h^{-1} for *E. coli* [42]. In newly born cells, it is postulated that Z ring formation is initiated from a single spot to form a ring. This process is rapid, requiring less than 1 min. During division, the Z ring decreases in diameter at the leading edge of the septum.

The pre-steady-state single turnover assays show that GTP hydrolysis is the major rate-limiting step (k hydrolysis $\gg$ 8/min) followed by the rapid release of phosphate (Pi) (k Pi release $\gg$ 8/min). At steady state, 80% of FtsZ polymer subunits are bound to GTP, and on GDP exchange with free GTP in solution [43,44]. The release of GDP might be partly rate-limiting and it happens either by direct nucleotide exchange in the polymers or via depolymerization and subsequent nucleotide exchange in the monomers. As noted by Romberg and Levin, a polymer composed of FtsZ-GTP is stable, whereas a hypothetical FtsZ-GDP polymer is likely to be metastable that favors depolymerization. In other words, a FtsZ-GDP polymer would be like a loaded spring that could disassemble rapidly, releasing the energy from many GTP hydrolysis events all at once. Polymer stability is directly affected by the rate of GTP hydrolysis, since FtsZ-GTP is stable, whereas FtsZ-GDP is the form that favors depolymerization [45].

2.2.3. Cytoskeleton ring or Z-ring

The Z ring is the heart of the division apparatus – it serves as the framework for the division apparatus and determines the site of cytokinesis. Z ring formation establishes the location of the future division site and is an integral part of the temporal regulation of cytokinesis. It has been proposed that the Z ring is positioned and assembled in response to the activation of a nucleation site at mid-cell. Consistent with this proposal, Z rings and spirals appear to grow bidirectional from a single point, suggesting that there is one nucleation site per Z ring. Also, immune staining for FtsZ reveals spots of fluorescence at early stages during the recovery of filamentous cells of a *ftsZ84* (Ts) mutant, indicating that Z rings are nucleated at single sites [46,47]. Formation of the Z ring acts as a significant portion of the cell cycle. In *B. subtilis* the proportion of cells with Z rings increases with increasing growth rate, implying that the Z period that means the time the Z ring is present in a given cell. It remains relatively constant even when doubling time decreases. The prolonged duration of the Z period suggests there may be a minimum time required for proper assembly of the entire division apparatus. There are no gross changes can be found in the Z ring during the Z period by immunofluorescence. The ring is extremely dynamic, with subunit turnover on par with that of the eukaryotic cytoskeleton [48].

When heat-sensitive *ftsZ* allele (*ftsZ84)* cells are raised to the non-permissive temperature, Z rings rapidly disassemble. After returning to the permissive temperature, FtsZ can reoccupy some sites but not those where invagination of the cell wall is visible. In *E. coli* formation of the Z ring, requires one of two proteins (ZipA or FtsA) that can tie up FtsZ protein to the membrane. Besides FtsZ, several other cell-division proteins are also involved in the dynamics of cytokinesis. Two new proteins designated FtsK and ZipA could participate at the level of division site recruitment. ZipA is an integral membrane protein that is essential for *E. coli* division. For instance, FtsA and ZipA appear to stabilize the Z-ring and ZipA is also involved in the crosslinking of FtsZ protofilaments, whereas SulA, EzrA, and MinC are inhibitors of FstZ polymerization [49].

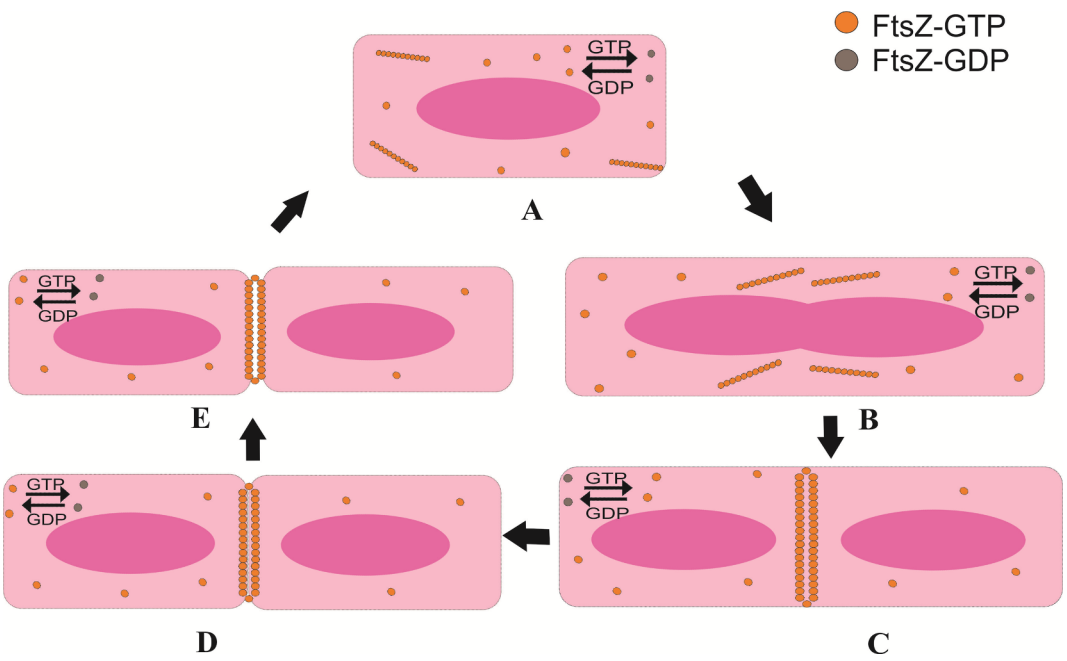

Fig. 2. Representation of Z-ring formation and cell division. (A) Bacterial cell prior to the onset of cell division with FtsZ protofilaments dispersed in the cell and undergoing continuous nucleotide exchange between GTP-bound FtsZ and GDP-bound FtsZ with rapid equilibrium, favoring GTP-bound FtsZ (B) Polymerization begins, cell elongation and, localization of FtsZ protofilaments at the mid-cell. (C) Generation of Z-ring: the 'steady-state turnover'-GTP hydrolysis in continuous competition with protofilament growth during polymerization. (D) Formation of septum (E) Contraction of the Z-ring followed by membrane alteration to bring about cell division.

3. FtsZ inhibitors

Abnormalities in polymerization and/or GTPase activity result in inhibition of the Z-ring and septum formation, leading to inhibition of cell division and cell death [6]. Several characteristics resume FtsZ as a target for the development of new antibacterial agent to selectively combat bacterial infections: (i) it is essential and plays a specific role in prokaryotic cell division; (ii) it is structurally and functionally conserved across bacterial and archaeal species but notably absent in higher eukaryotes; (iii) those antibacterial agents should not affect the host tissues and less chance of toxicity towards host cell. So a suitable antibacterial target in humans and (iv) there is a growing body of research on its structural, biochemical, and biological properties. Hence, compounds developed as FtsZ inhibitors must perturb either FtsZ polymerization or GTPase activity, or both. In this sense, the tightly regulated division process could be prohibited by mechanisms, like stabilization of protofilaments, so that it cannot hydrolyze GTP to form GDP or by preventing polymerization [50].

Several biochemical and cytological methods are used to assess the functional inhibition of FtsZ by small molecules. FtsZ polymerization has been extensively studied in vitro using basic methods including light scattering, sedimentation, GTP hydrolysis assays, and electron microscopy. A light-scattering assay determines the polymerized or bundling mass of FtsZ protofilaments [51]. The inhibition in the polymerization of the protein is reflected by a decrease in light scattering intensity. Meanwhile, a sedimentation assay can also be used to determine the effects of a compound on the polymer mass of FtsZ protofilaments [52]. In addition, the GTPase activity was measured by the Malachite green assay method. This assay (i.e., GTP hydrolysis assay) is used to measures the production of inorganic phosphate during GTP hydrolysis and assesses the effect of a compound on the GTPase activity of FtsZ. The isothermal titration calorimetry (ITC), saturation transfer difference NMR (STD-NMR) and an *in silico* molecular model is used to study the interaction of FtsZ inhibitors with their targets [53,54]. ITC provides a thermodynamic characterization of the specific molecular interactions associated with the binding reaction. STD-NMR spectroscopy and an *in silico* molecular model identify the epitopes of a compound that interact with FtsZ at atomic resolution. Furthermore, electron microscopy, transmission electron microscopy (TEM) and Immunofluorescence microscopy are used to visualize the change in morphology of FtsZ protofilaments and detection of Z-rings formation.

Given the importance of FtsZ assembly in cell division, it has been suggested as a putative antibacterial drug target, due to its evolutionary distance from eukaryotic tubulin. There are many efforts to identify inhibitors of FtsZ that do not target eukaryotic tubulin. Interestingly, most of the agents that target tubulin/microtubule, including paclitaxel, vinblastine, and colchicine, do not affect the dynamics of FtsZ assembly, indicating that the latter can be a selective antibacterial target [55]. The drug development in this criteria has been carried by design and synthesis numbers of new compounds and moderately high throughput (HTP) screening as well as rational optimization of the hit compounds. The compounds that interfere with FtsZ function can be classified on the basis of their mode of action on FtsZ or by their origin, natural or synthetic.

3.1. Natural products and semi-synthetic compounds

3.1.1. Curcumin

Curcumin **(1)**, a naturally occurring dietary polyphenolic compound extracted from the rhizomes of *Curcuma longa* exhibits potent antibacterial activity against a variety of pathogens, including Gram-positive and Gram-negative bacteria. Curcumin [1, 7-bis (4-hydroxy-3-methoxyphenyl)-1, 6-heptadiene-3, 5-dione/Diferuloylmethane], a hydrophobic polyphenol and its tautomeric form is shown in Fig. 3. The keto form of curcumin prevails in acidic and neutral media while enol form is stable and favored in alkaline media [56]. Curcumin is a yellow bioactive major component of turmeric, have been found to use as anticancer, antibacterial, antioxidant, etc [57]. Its rigid and electron-rich structure makes it an interesting candidate as a lead compound for further development of new inhibitors. Curcumin opposed the proliferation of gram-positive (*B. subtilis* 168) and gram-negative (*E. coli* K12MG1655 and *E. coli* BL21) bacteria with a MIC value of 100 μM for

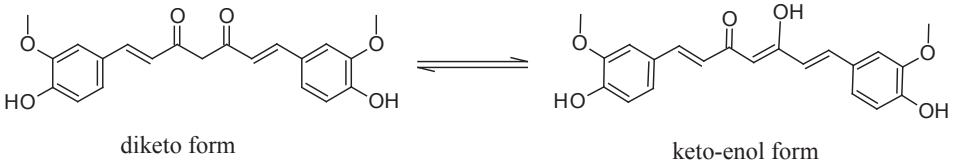

Fig. 3. Keto-enol tautomeric forms of curcumin (**1**).

B. subtilis 168. It induced filamentation in *B. subtilis* 168 cells which indicates that it inhibits bacterial proliferation by inhibiting cytokinesis without detectably affecting the segregation and organization of the nucleoids. Curcumin increases the 35% GTPase activity of FtsZ in the presence of 30 μM curcumin, indicating destabilization of FtsZ protofilaments [58]. Light scattering assay of curcumin was found to show that it reduced the light scattering intensity of polymerized mass of FtsZ protofilaments and hence bundling of FtsZ protofilaments was diminished. The decrease in intensity of polymerization and bundling of FtsZ may be due to the bulky nature of curcumin which affects steric hindrance. In an extensive study of the active site binding mode of curcumin reveals that the FlexX scores for selected docked poses in *E. coli* and *B. subtilis* FtsZ were −17.55 and −18.84 respectively [59]. The major site of binding to the active site in both proteins are keto-enol and one side of the terminal α hydroxyl group which plays an important role in FtsZ inhibition.

The docking study showed that keto-enol group and one side of the terminal hydroxyl group bind tightly to the active site of the both *B. subtilis* and *E. coli* FtsZ. Docked curcumin interact with most of the residues which were found to participate in GTP-binding. The binding interactions of curcumin deserve attention for designing more potent curcumin analogues with improved stability and bioavailability.

3.1.2. Cinnamaldehyde and its derivatives

Cinnamaldehyde (**2**), 3-phenylpropanoid chalcone, is the major constituent derived from the stem bark of Cinnamomum vernum. Cinnamaldehyde exhibited antibacterial activity with MIC value of 1 μg/ml for *E. coli*, 0.5 μg/ml for *B. subtilis* and 0.25 μg/ml for methicillin-resistant *Staphylococcus aureus* (MRSA) measured by broth microdilution method [60]. It strongly inhibited the light-scattering signal of FtsZ assembly and also showed inhibition of FtsZ GTPase activity in a dose-dependent manner with an IC50 of 5.81 ± 2.2 μM. Both nuclear magnetic resonance and an *in silico* docking model predicted the binding pocket cinnamaldehyde at the C-terminal region involving the T7 loop of FtsZ that perturbs the cytokinetic Z-ring formation.

Finding the potency of cinnamaldehyde, Li et al. carried out a novel program to design and synthesize a new library of cinnamaldehyde derivatives for screening against a variety of gram-positive and gram-negative bacteria (Fig. 4) [61]. The newly synthesized compounds generally displayed MIC values of 0.25–4 μg/mL against *S. aureus* ATCC25923. Especially, cinnamaldehyde derivatives containing a 2-methyl benzimidazolyl substitution at 1-position and phenyl (**3**), 2-chlorophenyl (**4**), 4-fluorophenyl (**5**), 4-chlorophenyl (**6**), 2, 4-dichlorophenyl (**7**), or 4-nitrophenyl (**8**) at the 3-position exhibited the most potent activity. In light scattering assay, compound **5** and **7** displayed the best activity in the various concentration range which indicated inhibition of FtsZ polymerization. In the GTPase assay, compound (**7**) showed 50% inhibition of GTPase activity at the concentration of 30 μg/mL and resulted in the instability of the FtsZ polymer, leading to the abnormal bacterial cell division. Compounds **(6)** and **(7)**

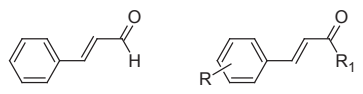

Fig. 4. Structure of Cinnamaldehyde and its derivatives.

with chlorine atom(s) at the 4- or/and 2-position of the benzene ring, implying that the substituents at both positions involved to the entire antibacterial activity. However compound **(5)** with the fluorine atom at the 4-position has the comparable activity to its 4-chlorine congener **(6)** and 4-methoxy derivative of compound **(9)** showed a decreased activity. The results of active cinnamaldehyde derivative compounds are representing novel scaffold and worthy of further investigation for potent FtsZ inhibitors.

3.1.3. Phenylpropanoids

Phenylpropanoids are the most distinct secondary metabolites found in plants and played an important role to defend plants against predators and pathogens [62]. The compounds belonging to this class have expressed to possess antibacterial properties and inhibit FtsZ. Hemaiswarya et al carried out assay on eight different phenylpropanoid compounds like cinnamic acid **(9)**, p-coumaric acid **(10)**, caffeic acid **(11)**, chlorogenic acid **(12)**, eugenol **(13)**, ferulic acid **(14)**, 3,4-Dimethoxycinnamic acid **(15)** and 2,4,5-Trimethoxycinnamic acid **(16)** against *Ec*-FtsZ and were found to inhibit FtsZ polymerization (IC50 69 μM to > 250 μM) (Fig. 5) [63]. Among eight phenylpropanoids, chlorogenic and caffeic acids showed a better result in GTP-induced FtsZ polymerization with IC50 of 70 and 106 μM, respectively assessed by a light-scattering assay. Under the polymerization conditions, chlorogenic acid at the concentration of 100 μM induced aggregation of FtsZ monomers and distorted protofilaments. In *B. subtilis* 168 cells, most of the phenylpropanoids were found to induce filamentation, indicating obstruction of bacterial proliferation by inhibiting cytokinesis. The studies involving the regulatory role of phenylpropanoids in FtsZ cell division could be considered as a new source for the development of antibacterial drugs in the future.

3.1.4. Plumbagin

Plumbagin (5-hydroxy-2-methyl-1,4-naphthoquinone) **(17)**, is a secondary plant metabolite derived from the root of *Plumbago zeylanica* exhibiting several biological activities, including its ability to inhibit proliferation of mammalian, fungal and bacterial cells (Fig. 6) [64,65]. Bhattacharya et al reported that plumbagin inhibited the proliferation of *B. subtilis* 168 and *M. smegmatis* cells [66]. It also disrupted the formation of functional Z-ring and induced the elongation of cell length of *B. subtilis* 168. It inhibited the growth rate of *B. subtilis* 168 cells in a concentration-dependent manner. The disruption of Z-ring formation in *B. subtilis* 168 cells indicated its polymerization of *B. subtilis* FtsZ (*Bs*FtsZ). Bhattacharya et al showed the extent of the assembly was reduced by 26, 33 and 45% in the presence of 2, 5 and 10 μM plumbagin, respectively. Plumbagin reduced the GTPase activity of *Bs*FtsZ at the rate of 2.5 and 1.7 mol Pi/mol FtsZ/ min in the absence and presence of 10 μM plumbagin, respectively. Interestingly, plumbagin did not inhibit either the assembly or GTPase activity of *E. coli* FtsZ in vitro which showed the difference in the structures of FtsZ proteins from different bacteria. Docking analysis indicated that the plumbagin binding site was located near the C-terminal of *Bs*FtsZ and interacted by hydrophobic and hydrogen- bonding interactions with *Bs*FtsZ. However, two residues in *Bs*FtsZ (aspartic acid at position 199 and valine at position 307) were found to be important for the binding interactions of plumbagin and *Bs*FtsZ. The results suggest that plumbagin inhibits

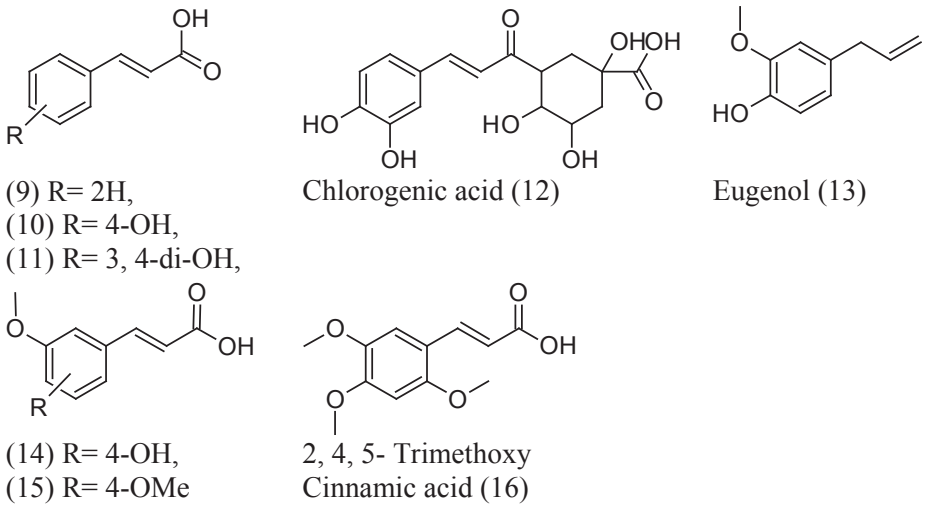

Fig. 5. Structure of Phenylpropanoids.

bacterial proliferation by inhibiting FtsZ assembly and contributes a rationale for developing potent plumbagin analogues.

3.1.5. Coumarins

Coumarins are the family of lactones containing benzopyrone skeletal framework, derived from plant sources [67]. It possesses a number of biological activities like analgesic, anti-inflammatory, antimicrobial, antiviral, antimalarial, anticoagulant, antioxidant, anticancer, etc. Duggirala et al screened some analogues of coumarins and reported the inhibition activities of the GTPase and polymerization against *E. coli* FtsZ (*Ec*FtsZ) protein effectively Fig. 7 [68]. Coumarins like scopoletin (**21**) inhibited FtsZ polymerization the best with an IC50 of about 41 μM followed by daphnetin (**22**) (72 μM). Both of the compounds inhibited the GTPase activity with IC50 values of 23 μM and 57 μM, respectively. Coumarin (**18**), 6-methylcoumarin (**19**), and 4-hydroxylcoumarin (**20**) showed less activity against GTPase and FtsZ polymerization (IC50, > 200 μM). TEM images of scopoletin and daphnetin indicated an aggregation of the monomers and hence block the formation of protofilament that leads to inhibition of polymerization. Coumarins such as umbelliferone (**23**), scopoletin (**21**) and phellodenol-A (**24**) inhibited the growth of *M. tuberculosis* H37Rv with MIC values of 58, 42, and 60 μg/mL, respectively [69]. Docking studies of *Ec*FtsZ showed that coumarins bind to T7 loop with the lowest binding energy is obtained with scopoletin. QSAR study reveals the need for groups such as hydroxyl, diethyl, or dimethylamino in the 7th carbon for enhanced activity. The promising results of coumarins justify the good selectivity against FtsZ protein.

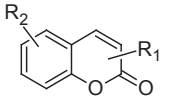

(19) R_1= 2H, R_2= 6-CH_3
(20) R_1= 2H, R_2= 4-OH
(21) R_1= 2H, R_2= 6-CH_3, 4-OH
(22) R_1= 2H, R_2= 7-OH, 8-OH
(23) R_1= 2H, R_2= 7-OH
(24) R_1, R_2= 6- CH_2 -CH_2-OH, 7-OH

(18) Coumarin R1, R2= 2H

Fig. 7. Structure of Coumarin and its analogues.

3.1.6. Totarol

Totarol (**25**), a diterpenoid phenol extracted from *Podocarpus totara*, native to New Zealand has been found to induce filamentation in *B. subtilis* cells and to inhibit bacterial cytokinesis (Fig. 6) [70]. At its minimum effective concentration (1.5 μM), totarol neither interrupted the membrane structure nor detectably influenced the nucleoid segregation in *B. subtilis* cells. But the disruption of the cytokinetic Z-ring indicating that at the same concentration, it inhibits bacterial cytokinesis by perturbing the formation and functioning of the Z-ring. Totarol was found to bind to *Mtb*FtsZ with a modest affinity (K_d) 11 ± 2.3 μM and inhibited the assembly and GTPase activity of *Mtb*FtsZ protofilaments by a change in conformation of the protein. It inhibited the GTPase activity of purified *Mtb*FtsZ by 50% in the presence of 40 μM totarol while it inhibited the growth of *B. subtilis* cells with a MIC of 2 μM. in vitro suggesting that it may serve as a lead compound for development of FtsZ targeted inhibitor.

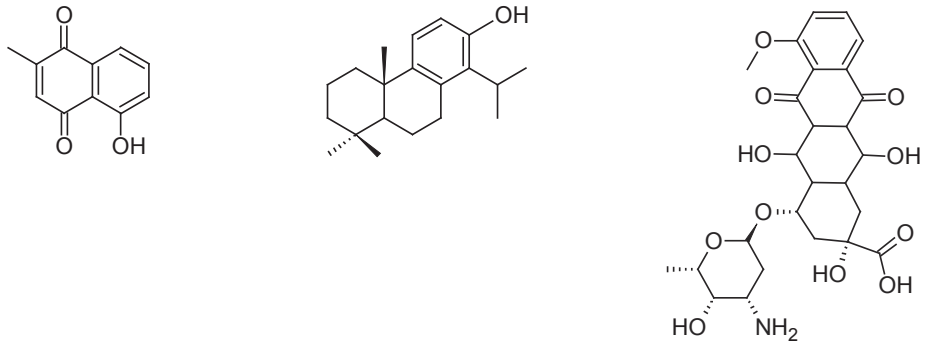

Fig. 6. Structure of Plumbagin (**17**), Totarol (**25**), Doxorubicin (**35**).

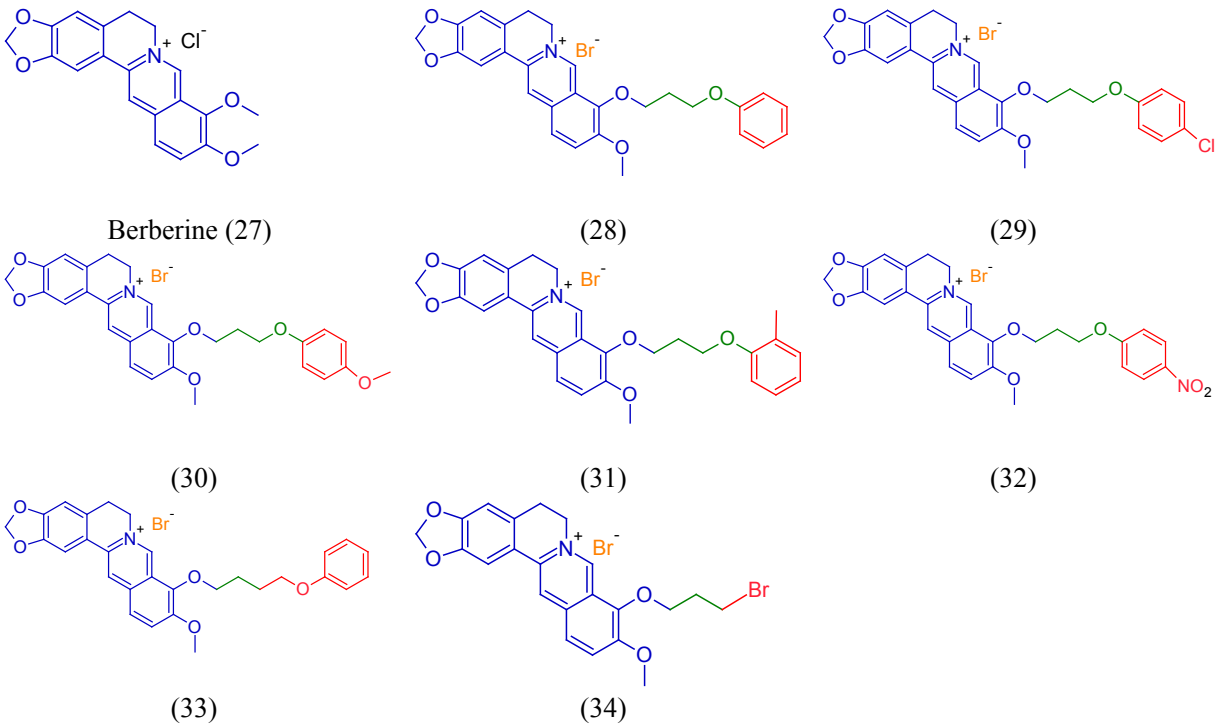

Fig. 8. Structure of Berberine and its derivatives.

The synthesis of heterocyclic analogues of totarol described by Kim and co-workers enabling indolototarol derivatives with enhanced antimicrobial activity. An advanced modification in A- ring with an indole ring and a carbon-to-nitrogen atom replacement on the B-ring made the totarol increased antimicrobial activity relative to the parent one but lack of activity in the enzymatic assay for FtsZ inhibition [71].

3.1.7. Sanguinarine

Sanguinarine (**26**) is a polycyclic alkaloid, derived from the rhizomes of *Sanguinaria canadensis*, that acts by inhibiting FtsZ protofilament assembly by decreasing FtsZ polymerization (Fig. 16) [72]. Beuria and co-workers demonstrated that sanguinarine inhibited cytokinesis in both Gram-positive and Gram-negative bacteria by arresting the *E. coli* FtsZ assembly. The IC50 values of sanguinarine against *B. subtilis* 168, *E. coli* BL21 (wild-type), and E. coli JM109 (WM647) were 1.0 ± 0.3, 4.6 ± 0.8, and 12.0 ± 1.7 μg/mL, respectively. It can also inhibit eukaryotic tubulin, which implies the harmful effect on mammalian cell [73]. The property of tubulin polymerization sanguinarine made it a drawback in the development of FtsZ inhibitor (see Fig. 17).

3.1.8. Berberine and its derivatives

Berberine (**27**) is an alkaloid isolated from various species of *Berberis*. It exhibits antibacterial activity against a variety of bacteria, including many pathogenic species and multidrug-resistant (MDR) strains of *M. tuberculosis* [74] and MRSA [75]. Domadia *et al.* reported a series of biological assays to investigate the mechanism of berberine and found to know that inhibited both FtsZ polymerization (IC50 10 ± 2.5 μM) and GTPase activity (IC50 16.01 ± 5 μM) in vitro, through light-scattering and GTP hydrolysis assays [76]. On the treatment of FtsZ polymer with berberine showed a decrease in length and bundling of Ftsz protofilaments causing destabilization which confirmed by Electron microscopy images. ITC result showed that the interaction of berberine with FtsZ occurred spontaneously and was driven by entropy with a dissociation constant of 0.02. *In silico* docking study with AutoDock software revealed the interaction of the dimethoxy groups, isoquinoline nucleus, and benzodioxole ring of berberine with FtsZ that proposed the putative binding site was in agreement with the STD-NMR.

By combining *in silico* structure-based design and in vitro biological assays, Sun et al design and synthesized a series of 9-phenoxy alkyl berberine derivatives as potent FtsZ inhibitors [77]. The antibacterial activity of 9-phenoxy alkyl-substituted berberine derivatives (**28**) to (**34**) inhibited the growth of antibiotic susceptible and antibiotic-resistant *S. aureus* strains with MIC values of 2–8 μg/mL as compared to MIC value of berberine 128–196 μg/ml (Fig. 8). On the other hand the growth of vancomycin-susceptible and vancomycin-resistant *E. faecium* were inhibited with MIC values of 4–16 μg/mL (berberine: 0.196 μg/ml) and the gram-negative strains of *E. coli* and *K. pneumoniae* were inhibited with MIC values of 32–128 μg/ml (berberine: 500 μg/ml). The presence of the aromatic ring in compounds (**28**) to (**34**) enhanced the antibacterial activity than Compound (**34**) without the 9-phenoxy group. Compounds (**28**) to (**34**) inhibited the GTPase activity of *S. aureus* FtsZ with relative IC50 values between 37.8 and 63.7 μM. The results of the GTPase inhibition assay suggest that the 9-phenoxy alkyl berberine derivatives establish stronger interactions with the FtsZ enzyme than the parent berberine. Additionally, the transmission electron microscopy showed that the Compound (**29**) (4 mM) reduced the thickness of the bundles of FtsZ protofilaments by 70% in *S. aureus* confirming the interruption of polymerization. Staining of *B. subtilis* membrane with the red fluorescent dye confirmed that compound (**29**) inhibits bacterial proliferation by inducing cell filamentation without perturbing the bacterial membrane. The studies clearly demonstrate that the chemical modification of berberine with 9-phenoxy alkyl derivatives significantly developed the antibacterial activity of FtsZ targeting protein.

3.1.9. Doxorubicin

The advances in techniques of isolation, screening, and profiling of compounds obtained from natural sources like plants and microbial fermentations make them more attractive and have been used as antibacterial agents. Doxorubicin, from a U. S. FDA, approved drug library using an independent computational, biochemical and microbial approach to identify small molecules targeting FtsZ and inhibiting bacterial division (Fig. 6) [78]. Doxorubicin (**35**), an anthracycline

Table 1
Antibacterial activity of Doxorubicin.

Strain	MIC (μM)	MBC (μM)
E. coli BL21	20	25
B. subtilis 168	10	15
S. aureus	5	5

Table 2
FtsZ sedimentation and GTPase activity of Doxorubicin.

	K_m (μM)	V_{max} (%)
Sedimentation	0.49 (0.31–0.66)	0.49 (0.31–0.66)
GTPase	0.72 (0.60–0.84)	0.72 (0.60–0.84)

antibiotic, isolated from an actinobacterium *Streptomyces peucetius* can hinder *E. coli* growth by perturbing FtsZ functions and was identified as a potent FtsZ inhibitor. The antibacterial activity of doxorubicin was found to be effective against all four strains of bacteria by determining MIC and MBC (minimal bactericidal concentration) using the CLSI guidelines (Table 1) [79]. Doxorubicin interacts strongly with FtsZ without affecting the membrane structure and nucleoid segregation in bacteria, shown by the fluorescence-binding assay. The number of proper Z-rings per cell was found to be 0.95 ± 0.1, 0.8 ± 0.2 and 0.2 ± 0.8 in the absence or presence of 20 μM and 40 μM doxorubicin respectively which clearly indicate that doxorubicin inhibits Z-ring formation and thus cell division in *E. coli* 10 μM concentration of doxorubicin inhibited GTPase activity by 27%which was similar to the decrease in the light scattering intensity (~25%), suggesting that both results are comparable. The *K*m values of 0.49 μM and 0.72 μM for sedimentation and GTPase activity respectively (Table 2) indicate that doxorubicin has similar effects on both FtsZ assembly and its GTPase activity. Furthermore, it was found that a number of single amino acid mutations at the identified binding site in FtsZ resulted in a several-fold decrease in the affinity of FtsZ for doxorubicin, recognizing the importance of this site for doxorubicin interaction. Identification of a novel binding site can be improved for the identification of newer and better FtsZ-targeted antibacterial agents.

3.1.10. Dichamanetin

The two natural polyphenolic compounds Dichamanetin **(36)** and 2‴-hydroxy-5″-benzylisouvarinol-B **(37)**, isolated independently by Hufford and Anam from *Uvaria chamae* and *Xylopia afticana* respectively, and are potent inhibitors of the GTPase activity of FtsZ (Fig. 9) [80]. This two natural products dichamanetin and 2‴-hydroxy-5″-benzylisouvarinol-B from a common core structure using a new zinc chloride-mediated benzylic coupling reaction. Dichamanetin was efficiently synthesized from pinocembrin as starting material by a zinc chloride-mediated benzylic coupling reaction. Both of the compounds are potent inhibitors of *E. coli* GTPase activity. The IC50 Dichamanetin (12.5 ± 0.5 μM) and 2‴- hydroxy-5″-benzyliso-uvarinol-B (8.3 ± 0.5 μM) indicates that these compound are active towards bacterial cell division protein FtsZ.

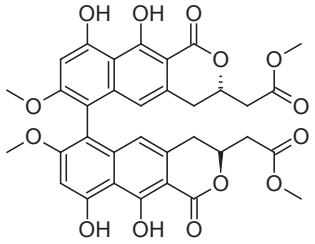

Viridotoxin (38)

Fig. 10. Structure of Viridotoxin (**38**).

3.1.11. Viriditoxin

Viriditoxin **(38)**, obtained from *Aspergillus viridinutans*, was first reported in 1971, but its structure was incorrectly assigned at that time and was corrected in 1990 (Fig. 10) [81]. Viriditoxin was identified as FtsZ inhibitor from a pool of more than 100,000 extracts of microbial fermentation broths and plants followed by fractionation using fluorescent FtsZ polymerization assay [82]. It was confirmed to block *E. coli* FtsZ polymerization with an IC50 of 8.2 μg/ml and concomitant GTPase inhibition with an IC50 of 7.0 μg/ml. Viriditoxin did not exhibit inhibitory activity against DNA, RNA, protein, fatty acid, or cell wall biosynthesis. Furthermore, viriditoxin exhibited broad-spectrum antibacterial activity against many clinically relevant Gram-positive pathogens, which indicated high functional conservation of FtsZ in these clinically important species. It showed a MIC value of 4–8 mg/mL for various strains of *S. aureus* and MIC value 2–16 mg/ml for various strains of *Enterococcus faecalis* and *Enterococcus faecium*. The result of MIC and IC50 of viriditoxin showed there is an interaction with FtsZ protein. Yet the presence of highly conserved protein at the viriditoxin binding site may lead to restriction of FtsZ to develop resistance to this drug. Although viriditoxin may not be a drug itself, it could be a lead molecule that further modification of its structure could help in the development for drug discovery as well as a vital role in the field of cell division.

3.2. Synthetic small molecules

3.2.1. Guanine nucleotide

It has been shown that FtsZ polymerization and GTP hydrolysis to guanosine diphosphate (GDP) is crucial for the integrity of the Z-ring. FtsZ polymerizes at the GTP binding site to form protofilaments. Structurally FtsZ and tubulin share a similar three-dimensional structure, which possesses the same amino acid sequence for GTP binding and hydrolysis. These facts visible to design GTP analogues selective to the prokaryotic protein FtsZ acts to be a challenging job. La¨ppchen and co-workers designed a selective inhibitor of FtsZ based on the structure of its natural substrate GTP **(37)** and reported the inhibitory activity of

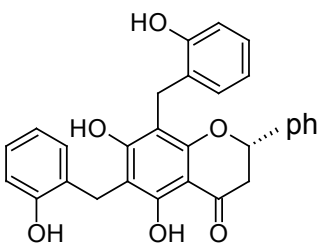

Dichamanetin (36)

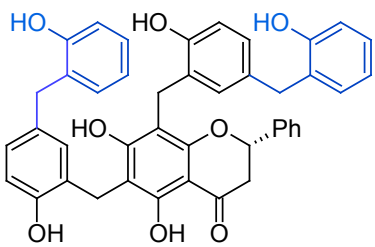

2‴- hydroxy-5″-benzyliso-uvarinol-B(37)

Fig. 9. Structure of compound (**36**) and (**37**).

8-bromoguanosine 5′- triphosphate (BrGTP) **(38)** [83]. The inhibitory properties were characterized by both electron microscopy and a coupled assay, which shows simultaneous identification of the extent of polymerization via light scattering and GTPase activity via the release of inorganic phosphate. BrGTP and GTP compete for binding of soluble FtsZ but the IC50 for GTPase activity in the ratio of 1:1 (BrGTP: GTP) suggests that equal binding affinity of both nucleotide, resulting in inactive of BrGTP-FtsZ. Interestingly on 2-fold excess addition of BrGTP, FtsZ was fully polymerized and resulted in complete depolymerization and inhibition of GTPase activity within 5 s. The result demonstrated that BrGTP acts as a competitive inhibitor of both FtsZ polymerization and GTPase activity and showing Ki value of 31.8 ± 4.1 μM for GTPase activity [83]. It could also affect polymer destabilization by directly replacing GTP/GDP in the polymers. From this, it indicates that BrGTP does not inhibit tubulin assembly due to the difference in GTP binding site of FtsZ and tubulin.

La¨ppchen and co-workers designed a structurally diverse series of C8-substituted GTP analogues **(38)** and reported their actions on both FtsZ and tubulin along with the description of their binding to FtsZ by protein crystallography [84]. Their mode of action was determined by a fluorescent competition assay with 2′/3′-O-(*N*-methyl-anthraniloyl)-guanosine-50-triphosphate (mantGTP) and showed more potent inhibition of both FtsZ polymerization and the associated GTPase activity [85]. The series of C8-substituted GTP analogues showed tubulin assembly-promoting effects include a reduced lag time before assembly, a steeper slope, and a higher final level of turbidity increase/decrease in a parallel fashion in the series GTP < IGTP < MeOGTP < BrGTP < ClGTP by employing a common turbidity assay (Fig. 11). The C8-substituted GTP analogues are better substrates of the tubulin GTPase than GTP, strongly indicating that similar to FtsZ, 8-RGTPs compete with GTP for binding to the exchangeable nucleotide-binding site of tubulin (E site). These C8-substituted GTP analogues show antibacterial effect probably due to their poor penetration across the bacterial cell (Table 3) [84].

Filipa Marcelo et al investigated the molecular recognition of C8-substituted guanine nucleotides eg. 8-Morpholino-GTP (MorphGTP), 8-Morpholino-GMP (MorphGMP), 8-pyrrolidino-GDP (PyrrGDP), 8-pyrrolidino-GMP (PyrrGMP), MethoxyGTP (MeOGTP) and MethoxyGMP (MeOGMP) by combining NMR techniques with biochemical and molecular modeling procedures by FtsZ from *Methanococcus jannaschii* (*Mj*FtsZ) and *Bacillus subtilis* (*Bs*FtsZ). GMP interacts in the same anti conformation as GTP, whereas 8-pyrrolidino-GMP binds in the syn conformation [86]. Although both anti- and syn conformation of 8-morpholino-GMP is selected by *Mj*FtsZ while *Bs*FtsZ binds only anti conformation. As Morph GTP behaves as a nonhydrolyzable analogues, its binding induces formation curved filaments whose binding, resembling polymers formed by the inactive forms of this protein. The C8-

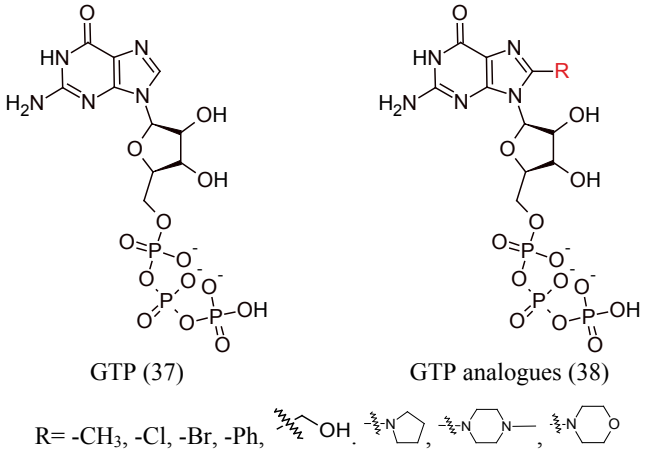

Fig. 11. Structure of C8-substituted guanine nucleotides.

Table 3
Inhibition activities of C8-substituted GTP analogues.

Nucleotides	IC50 polymerization (μm)	IC50 GTPase (μm)	GTP hydrolysis (%)
GTP	–	–	90.8 ± 3.4
MeGTP	44	52 ± 5.7	na
ClGTP	35	44 ± 3.4	44.2 ± 0.7
BrGTP [56]	37	60.2 ± 8.8	59
PhGTP	71	na	72
MeOGTP	10	15.3 ± 0.4	5.9
PyrrGTP	15	21.4 ± 0.9	16.6
MorphGTP	139	179 ± 15	77.9
NMePipGTP	252	298 ± 33	87.7
NMePipGTP	252	298 ± 33	87.7

na: not available.

Substituent acts by inducing electrostatic remodeling and small structural displacements at the association interface between FtsZ monomers to form filaments, that causes complete assembly inhibition or to the generation of abnormal FtsZ polymers.

3.2.2. Zantrins

In a high throughput protein-based chemical screen of 18,320 compounds, Margalit et al reported the identification of five structurally diverse compounds, named 'zantrins' (Z1, Z2, Z3, Z4, Z5) **(39–43)** that target assembly-dependent GTPase activity of FtsZ (Fig. 12). The IC50 of each zantrin was determined by using the malachite green-phosphomolybdate colorimetric assay. In this assay, GTPase activity was measured by the release of inorganic phosphate upon GTP hydrolysis. The inhibition GTPase activity of *E. coli* FtsZ showed in the range of 4–25 μM and M. tuberculosis FtsZ with 30–70 μM (Table 4) [87]. The electron microscopy and quantification of effects of Zantrins on steady-state FtsZ polymer mass and structure indicated that Zantrins inhibited FtsZ GTPase either by destabilizing effect of these compounds on polymer assemblyZ1 **(39), Z2 (40)** and Z4 **(42)** or by inducing filament hyperstability of Z3 **(41)** and Z5 **(43)**. Margalit *et al.* explained the destabilizing Zantrin may bind to a pocket between FtsZ subunits such that the synergy loop T7 in one surface of FtsZ monomer fails to make optimum contact with the GTP bound to loops T1–T6 in the neighboring monomer stimulating GTP hydrolysis which is essential for FtsZ polymerization.

In contrast, the stabilizing Zantrins could inhibit FtsZ depolymerization by opposing the movement of the switch loop T3 that has been proposed to cause a bend in the filament upon GTP hydrolysis. The results from immunofluorescence microscopy demonstrate that Zantrins perturb Z ring assembly in *E. coli* cells by directly targeting FtsZ in vivo, without exerting any major effect on chromosome segregation. These Zantrins also inhibited the recruitment of ZipA and FtsA as the stabilizing factors for Z-rings in vivo and were lethal to a range of organisms in broth culture including antibiotic-resistant and virulent pathogens. As compared to other Zantrins, Z1 **(39)** was broadly cell-permeable and displayed significant potency against Gram-positive organisms, further supporting the hypothesis that FtsZ is a good target for the development of new broad-spectrum antibacterial agents.

3.2.3. Benzamide derivatives

The most desirable reported studied on FtsZ inhibitors are the benzamides analogues, a family of synthetic 3-methoxy benzamide (3-MBA) **(44)** an attractive starting point for the discovery of potent FtsZ inhibitors (Fig. 13). It acts by disturbing either the polymerization or the GTPase activity with minimum inhibitory concentration (MIC) values of 4000 μg/ml against *B. subtilis* [88]. Because of its low molecular weight, it is able to penetrate the bacterial cell and binds to FtsZ at high ligand efficiency, which makes 3-MBA an attractive starting point to design more efficient FtsZ inhibitors [89]. Instead of amide and 3-ether substituents of 3-MBA, an extension of the 3-alkyloxy substituent

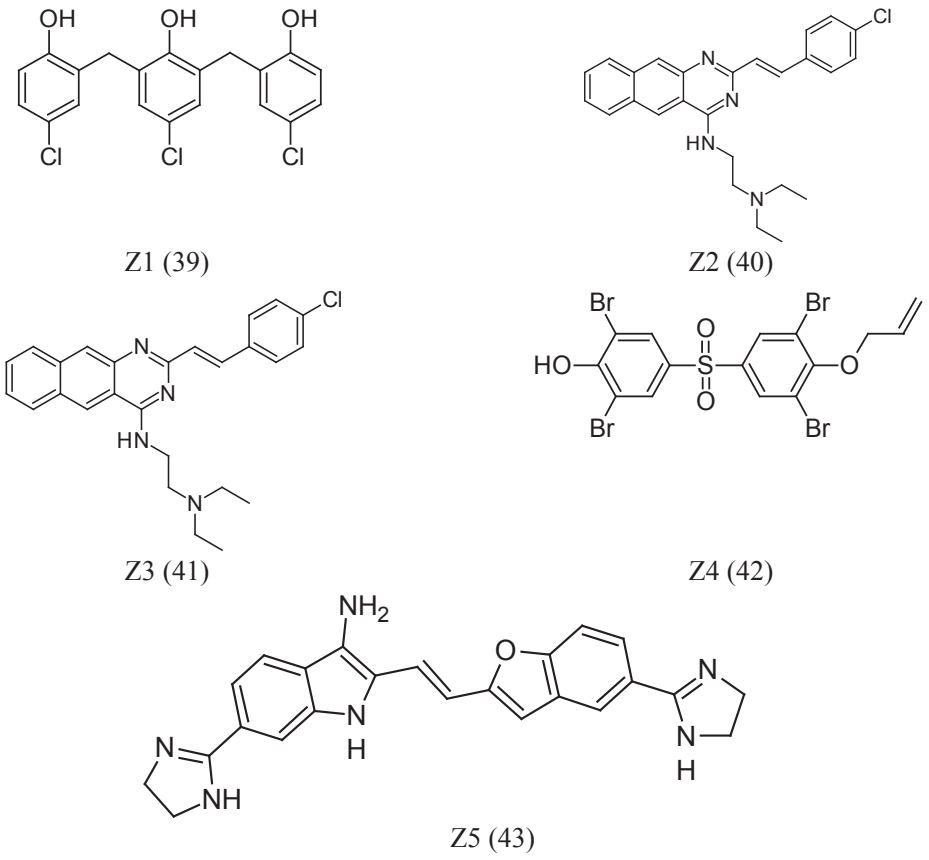

Fig. 12. Structures of Zantrins.

Table 4
Antitubercular and antienterococcal activities of zantrins.

Zantrins	IC50, μM	
	FtsZ *Ec*	FtsZ *Mtb*
Z1	5	55
Z2	10	70
Z3	15	50
Z4	25	> 100
Z5	4	30

improved antibacterial activity and led to the identification of compound 46 with on-target activity and MICs of 0.5 and 2 μg/ml against *B. subtilis* and *S. aureus*, respectively. On account of its good ligand efficiency with on-target, many scientists focussed on designing of various analogues of 3-methoxy benzamide. Recently identification of PC190723 **(45)**, one of the synthetic analogues of 3-methoxy benzamide is characterized by substituted benzamide and thiazolopyridine moieties joined together via an ether linkage [90]. It was found to possess potent activity against *B. subtilis* with a MIC value of 0.5–1.0 μg/ml by inhibiting FtsZ GTPase activity in vitro. By electron microscopy analysis, PC190723 **(45)** (2 μg/ml) on *S. aureus* showing cell enlargement and killing of staphylococci in vivo [91]. The replacement of thiazolopyridine with a benzothiazole group in PC190723 displays more potent activity with a MIC value of 0.25 μg/ml against *S. aureus* than PC190723 [92]. The structure-activity relationship shows that 3-methoxy group with various moieties such as alkyl, aryl or heteroaryl groups results in drug-like 3-MBA derivatives with on-target antibacterial activity instead of critical for cell division inhibition of amide and the 3-methoxy group of 3-MBA **(44)** [93].

Crystal structure of *S. aureus* FtsZ (*Sa*FtsZ) bound with PC190723 seemed to be related to the polymerization state by sliding/rotation between two subdomains with a concomitant conformational change of the T7 loop [94]. Hence, the SaFtsZ structure has been postulated as representing a straight protofilament conformation, while other structures are curved (and relaxed) conformations. Recent co-crystal structures of PC190723 and *Sa*FtsZ have confirmed that the benzamides bind within a deep hydrophobic cleft formed between the H7 helix and the C-terminal subdomain in close proximity to the T7 loop [95]. However, the inhibitory activity and most remarkable improvement in on-target activity due to reasonably long hydrophobic side chain and a preferred terminal group will support for the interaction with the hydrophobic cleft.

Siti ma et al. [96] followed up a further optimization of 3- methoxy benzamide derivatives in order to get better candidate drugs. In contrast, the subseries of 3-phenoxyaklyloxybenzamide, 3-heteroaryl alkyloxy benzamide and 3-heteroaryl thioalkyloxy benzamide derivatives of compounds had a remarkable improvement in antibacterial activity and on-target against *B. subtilis*. Among all of the tested compounds, 4-chlorophenyl derivative **(48)** (0.25 μg/ml) had the most potent antibacterial activity against *B. subtilis* ATCC9372 and 3-butoxypentyloxy derivative **(47)** presented the best antibacterial activity against resistant *S. aureus ATCC29213*. Stroke et al carried out an investigation on designing, synthesis of various analogues of oxazole-benzamide inhibitors of bacterial cell division protein FtsZ. The presence of a phenyl-substituted oxazole heterocycle in place of the thiazol pyridine of PC190723 and substitutions at the pseudo- benzylic position of the linker between the benzamide and oxazole moieties were significantly improving the target activity. The analogues possessing a 5-halo oxazole derivative such as **(49)** markedly enhanced potencies against wild-type *S. aureus*, with MICs as low as 0.03 μg/ml. In addition, substitutions at the pseudo-benzylic position provided the possibility of

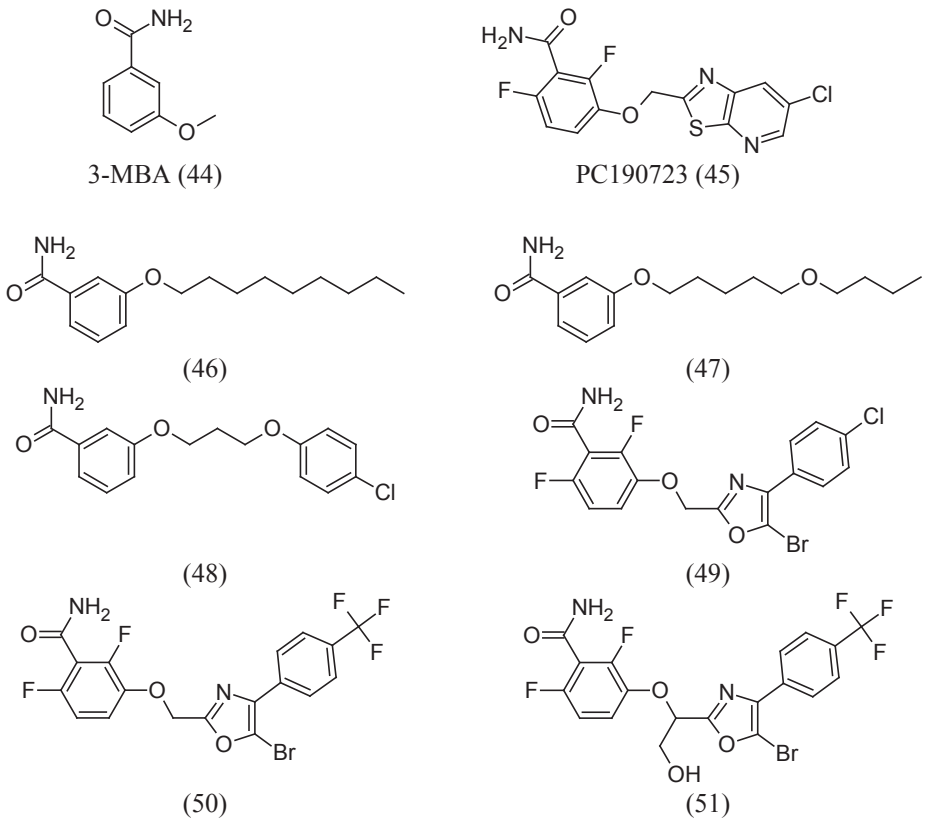

Fig. 13. Structure of Benzamide derivatives.

increasing the solubility of the compounds either by increasing the intrinsic solubility of the parent molecule or by providing a handle to introduce pro-drug functionality via an ester linkage. The kinetic solubility of compound (**36**) was increased markedly by 100 μg/ml, compared to 12.5 μg/ml of the unsubstituted analogue, shown in compound **(50)** at neutral pH. However, pseudo-benzylic substituted analogues exhibited ideal pharmacokinetic properties like AUCs, half-lives and clearance rates, especially, the hydroxymethyl-substituted analogue **(51)**.

But the clinical development of PC190723 has been obstructed by poor drug-like and pharmacokinetic properties. So the development and designing of two prodrugs of PC190723, TXY436 and TXY541 (**52 and 53**) resulted significantly increased pharmaceutical properties with better intravenous efficacy as well as the first demonstration of oral efficacy in vivo against both *methicillin-sensitive Staphylococcus aureus* (MSSA) and *methicillin-resistant S. aureus* (MRSA) (Fig. 14) [97]. In spite of capable of producing an intended result in vivo, the doses required for efficacy were high and suboptimal pharmacokinetic properties. Hence to improve the metabolic stability and pharmacokinetic properties, Malvika Kaul et al. designed a new prodrug TXA709 **(55)** in which the Cl group on the pyridyl ring has been replaced with a CF3 functionality that is resistant to metabolic attack [98,99]. The superior in vivo antistaphylococcal profile of the TXA709 **(55)** prodrug TXA707 **(54)** (Fig. 14) is associated with enhanced efficacy relative to TXY541 **(53)** against systemic infections with either MSSA or MRSA. The potency of orally administered TXA709 **(55)** against MRSA in the mouse tissue model of infection showed that ~2-log reduction in bacterial CFU relative to vehicle-treated mice ($P \leq 0.003$) at 24 h post-infection as compared to ~0.5-log reduction in bacterial CFU on oral administration of 200 mg/kg every 6 h over a 24-h period in case of PC190723. Furthermore, the efficacy of TXA709 **(55)** against mammalian cytotoxicity was got to manifest less toxic to both human cervical cancer (HeLa) and Madin-Darby canine kidney (MDCK) cells, with 50% inhibitory concentrations (IC50s) of ≥120 μg/ml. PC190723 is a class of arylalkyloxybenzamides that represent a remarkable improvement in on-target activity and further its clinical development lead to design prodrug TXA709 **(55)** with enhanced metabolic stability, improved pharmacokinetic properties, less cytotoxicity to mammalian cells and superior in vivo efficacy versus MRSA. So it is considered as an excellent lead compound to build into a clinically useful agent for the treatment of drug-resistant staphylococcal infections.

To further investigate on a reduction of the drug dose, drug-induced toxicity and potential for the emergence of resistance, Kaul and their coworkers developed a combination therapeutic approach for treatment with TXA709 **(55)** [100]. The combination of TXA709 **(55)** with the third-generation oral cephalosporin, cefdinir was found to show 3-fold reduction in the oral dose of TXA709 **(55)** required for efficacy and minimize the rate of occurrence of resistance in MRSA, vancomycin-intermediate *S. aureus* (VISA), vancomycin-resistant *S. aureus* (VRSA), and linezolid-resistant *S. aureus* (LRSA). The MIC of synergistic activities of TXA707 **(54)** and cefdinir against clinical isolates of MRSA, VISA, VRSA, and LRSA was reported to range from 0.125 to 0.25 μg/ml, done by Microdilution assays with cation-adjusted Mueller-Hinton (CAMH) broth. The checkerboard titration method was employed to evaluate synergy between TXA707 **(54)** and cefdinir against MRSA, VISA, VRSA, LRSA, and MSSA isolates and determined Fractional Inhibitory Concentration Index (FICI) of ≤ 0.375, confirming synergy effect.

As staphylococcal infections usually happen in soft tissue, the synergistic actions of orally administered TXA709 **(55)** and cefdinir in a mouse tissue (thigh) model of infection with MRSA ATCC 33,591 was examined. The result showed a 4-log reduction in the bacterial CFU count on a combination of 40 mg/kg TXA709 **(55)** and 200 mg/kg cefdinir, in contrast to a 1-log reduction in the bacterial CFU count by oral administration of 40 mg/kg TXA709 **(55)** and 200 mg/kg cefdinir individually. The collective shreds of evidence focus the most prospective FtsZ targeting TXA709 **(55)** and cefdinir combination to treat drug-resistant staphylococcal infections.

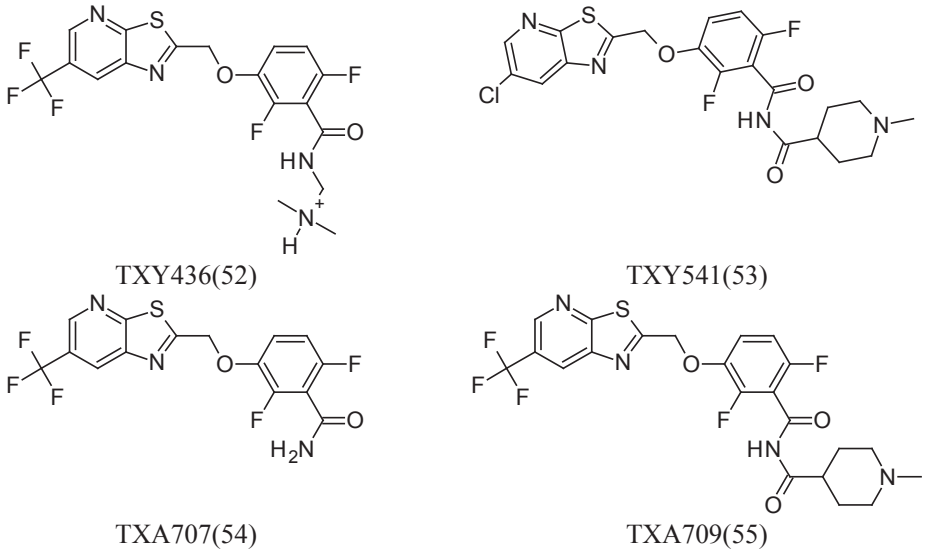

Fig. 14. Structure of prodrugs of PC190723.

3.2.4. 2-alkoxycarbonylpyridine and 2-carbamoyl pteridine

White et al. reported that a library of thousand 2-alkoxycarbonylpyridine analogues was designed at the Southern Research Institute (SRI) and screened as polymerization inhibitors [101]. More about 200 compounds from the SRI repository were submitted to the Tuberculosis Antimicrobial Acquisition and Coordinating Facility (TAACF) for screening and from them, two molecules SRI-3072 **(56)** and SRI-7614 **(57)** were selected for advanced studies (Fig. 15).

The MIC_{99} of SRI-7614 **(57)** and SRI-3072 **(56)** were determined for drug-resistant *M. tuberculosis* through the TAAC using a colorimetric (Alamar Blue) microdilution broth assay and were found to be 6.25 and 0.15 mg/L respectively. The MBC of both that is the lowest drug concentration that reduced the CFU by 2 log10 ± S.D. ($n = 4$) were also determined to find their bactericidal properties. The result of the ratio of MIC to MBC of SRI-3072 **(56)** was coming 4 and considered as bactericidal using a value for the MIC and MBC of 0.47 μM and 1.9 μM.

SRI-3072 **(56)** and SRI-7614 **(57)** inhibited *M. tuberculosis* FtsZ polymerization in a dose-dependent manner, with ID50 values of 52 ± 12 and 60 ± 0 by using light scattering assay method. And also 100 μM of SRI-3072 **(56)** and SRI-7614 **(57)** were showing inhibition of GTP hydrolysis by 20 and 25%, respectively. Since FtsZ and tubulin share the same GTP binding motif and have sequence similarity (less than20%), the effect of the two compounds on inhibition of tubulin polymerization was also calculated. Table 5 is representing SRI-3072, SRI-7614 and two other 1-deazapteridines (SRI-5713**(58)** and SRI-20158 **(59)**) as inhibitors of GTP hydrolysis and tubulin

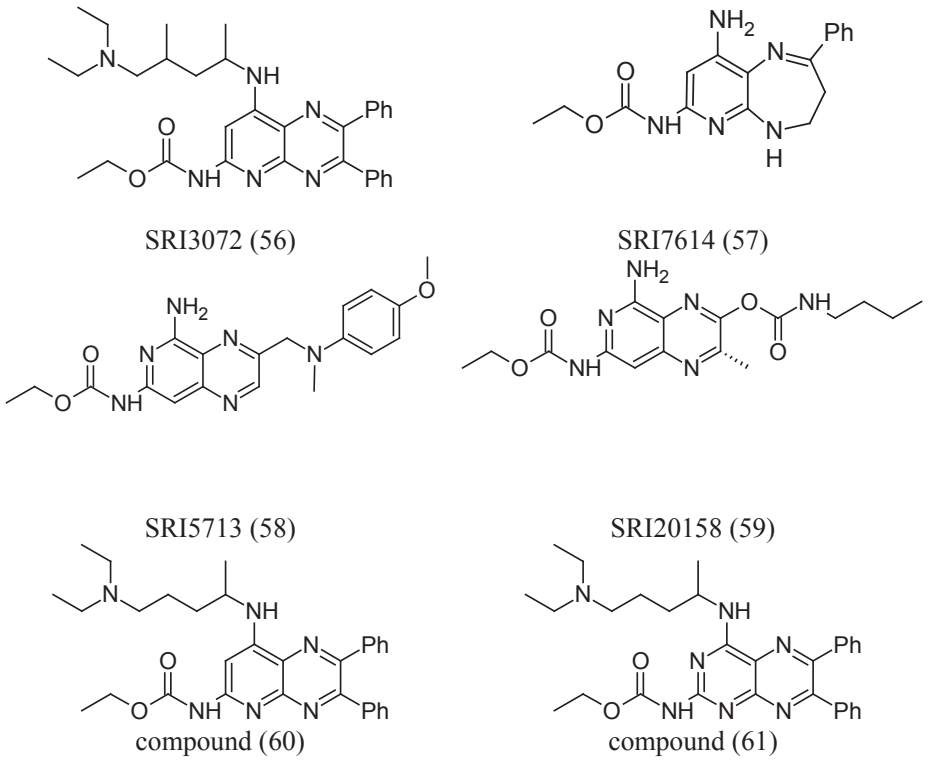

Fig. 15. Structure of 2-carbamoyl pteridine (**56**) to (**61**).

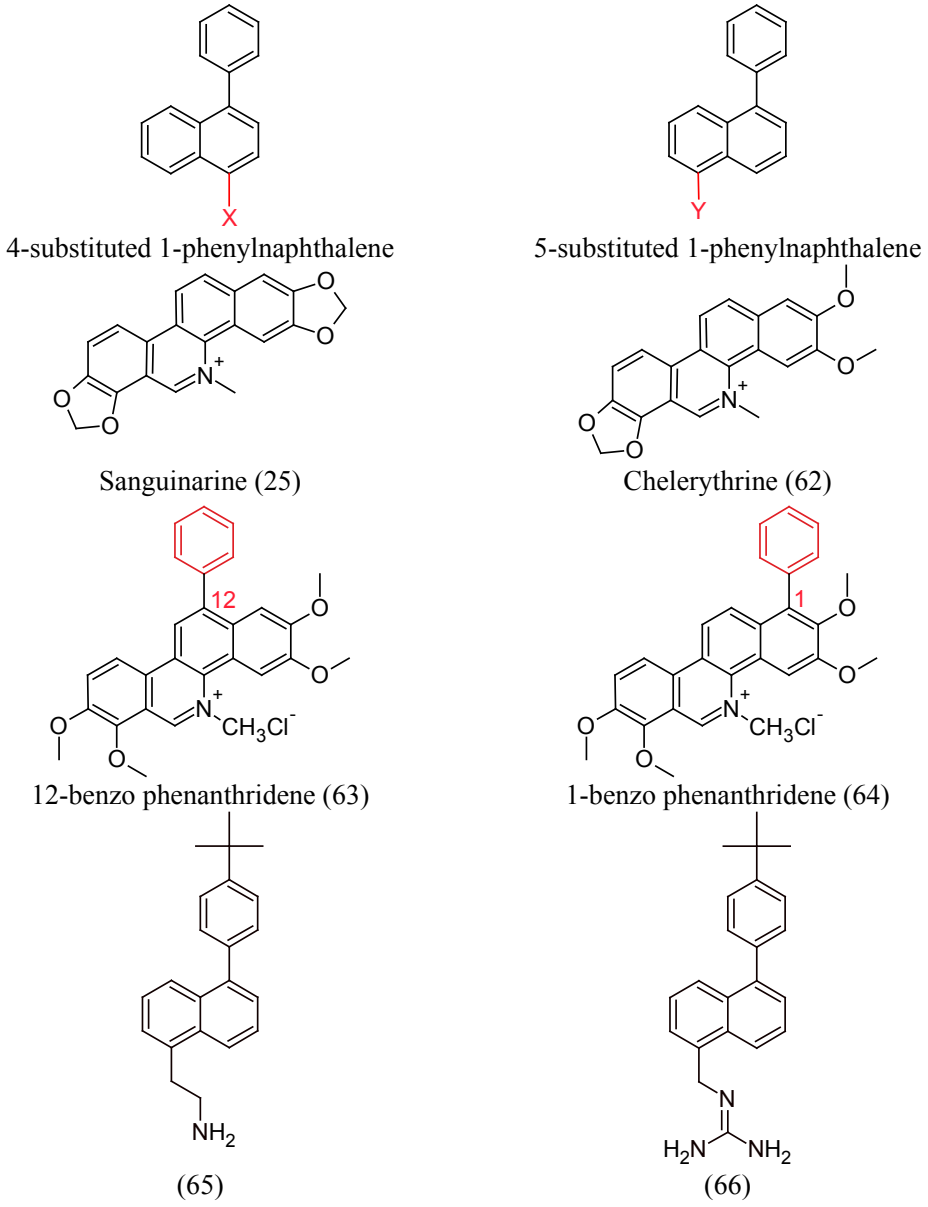

Fig. 16. Structure of compound (**25**) and (**62**) to (**66**).

polymerization. As *M. tuberculosis* is an intracellular parasite, SRI-3072 **(56)** has also the property to enter macrophages readily and reduced the growth of *M. tuberculosis* Erdman in macrophages. The favorable result of polymerization and GTP hydrolysis of *M. tuberculosis* FtsZ made the development of SRI compounds toward clinical candidates.

From a drug design point of view, SRI-3072 **(56)** generally fit the acceptable range of orally active and drug-like properties based on Lipinski rule of five. But slightly weight over 500 leads to a modification to improve its target activity. Besides that, it can readily form hydrochloride salts that will alter its solubility and permeability of compound.

The 3-deazapteridine nucleus is an acceptable pharmacophore to give a new design to overcome its drug-likeness properties and allowing the ready and inexpensive preparation of various analogues for a structure-activity relationship [102]. The modified analogue of pteridine nucleus (**61**) showed MIC for *M. tuberculosis* H37Ra 2 μg/ml, eight-fold lower than SRI-3072 **(56)** using a colorimetric (Alamar blue) microdilution broth assay. The compound is fully potent in inhibiting *Mtb* FtsZ polymerization and GTP hydrolysis (Table 6). The degree of efficiency of preparing these types of analogues with a good percentage of yield and inhibition of polymerization suggesting the acceptable substitution of pteridine nucleus. The inhibitory activity of 3-deazapteridine analogues provides convincing confirmation that the inhibition of FtsZ polymerization is a novel drug target that assures further research focus.

3.2.5. 4-Substituted and 5-substituted 1-phenyl naphthalene

Sanguinarine **(25)**, chelerythrine **(62)** and it's analogue (1-phenyl 2,3,8,9-tetramethoxy-5- methylbenzo[*c*]phenanthridinium chloride) **(63** and **64)** (Fig. 16) were identified as a small molecule of FtsZ-targeting antibacterial agents can alter Z-ring formation by either enhancing or inhibiting FtsZ self-polymerization [103]. The presence of hydrophobic functionality at either the 12- or 1-position of benzo[*c*] phenanthridines exert enhanced antibacterial activity. Constitutive cationic charge on their structure can adversely influence their desired pharmacokinetic properties. So, to overcome this effect, Kelley et al. designed and synthesized a series of 4- and 5-Substituted 1-phenyl naphthalenes which represent a truncated form within the core structure with a lack of constitutive cationic charge [104].

The MIC value of all the compounds showed 0.5–16 μg/ml against the methicillin-sensitive and resistant *S. aureus* as well as vancomycin-

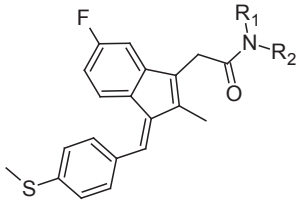

Compounds	R1	R2	MtbH$_{37}$Rv IC90 (μM)
(67)	H	$CH_2CH_2N(CH_3)_2$	7.29±0.23
(68)	H	-$CH_2CH_2CH_2N(CH_2CH_2CH_2CH_3)2$	0.85±0.00
(69)	CH3	-CH_2CH_2NH-CH_3	8.28±0.33
(70)	H	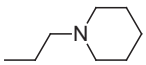	1.41±0.03
(71)	H	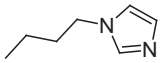	1.18±0.01
(72)	H	benzyl	>100
(73)	H	4-(N, N-dimethylamino)benzyl	>100
(74)	H	Furan-2-ylmethyl	>100

Fig. 17. *M. tuberculosis* H37Rv cytotoxicity data of compound (**67**) to (**74**).

Table 5
Polymerization and GTP hydrolysis of *Mtb* FtsZ inhibitors.

Compound	*Mtb*FtsZ	
	polymerization ID50 (μM)	GTP hydrolysi [% inhibition (100 μM)]
SRI3072 (56)	104 ± 2	35
SRI7614 **(57)**	52 ± 12	20
SRI5713 **(58)**	No inhibition	ND
SRI20158 **(59)**	No inhibition	ND

Table 6
The activity of compound **60** and **61**.

Compounds	*Mtb* FtsZ	
	Polymerization ID50 (μM)	GTP hydrolysis
(60)	34.2 ± 2.5	35% at 100 μM
(61)	38.1 ± 4.1	23% at 200 μM

sensitive and resistant *E. faecalis* (vancomycin-resistant *enterococci*) VRE, were conducted in accordance with Clinical Laboratory Standards Institute (CLSI) guidelines for broth microdilution than the clinical antibiotics evaluated in this study. Compound **66** was most active against MSSA with a MIC of 0.5 μg/ml while compound (**65**) with a MIC of 2 μg/ml. Eventually, Polymerization of *Sa*FtsZ was monitored using a microtiter plate-based turbidity assay. Compounds (**65**) and (**66**) were found to show the extent of *Sa*FtsZ polymerization. The FtsZ polymerization suggests that the antibacterial activity of the phenyl naphthalene is associated with the stimulatory impact of the compounds on the dynamics of FtsZ polymerization.

3.2.6. Sulindac

Enlightened by an indomethacin analogue closely related to sulindac sulfide amide (SSA), Mathew et al. reported the activity of sulindac analogue series against *Mtb* FtsZ polymerization [105]. The screening of sulindac analogues was performed against *M. tuberculosis* H37Rv to determine the IC90 (the concentration that inhibits bacterial growth by 90%) using a colorimetric (Alamar blue) microdilution broth assay. The presence of basic acyclic acetamide linker at the C-3 position of Sulindac sulfide exhibited potency activity center against *M. tuberculosis* H37Rv strain. The compound (**68**) having two *n*-butyl groups at the terminal nitrogen was found to show significant activity than the compounds substituted with methyl and ethyl groups (Fig. 17). Besides piperidinyl ethyl (**70**) and imidazole-1-ylpropyl (**71**) substituted sulindac sulfide amide displayed more relevant in *Mtb* whole-cell activity. But the compounds with aromatic (**72, 73**) or heteroaromatic (**74**) groups at the acetamide linker are inactive in the assay (Fig. 17). On the expansion of the study of the activity of sulindac analogues, benzothiazole-2-ylmethylene group at the C-1 position compound (**75**) to (**79**) (Fig. 18) showed significant activity against *M. tuberculosis* H37Rv that was comparable to their 4-methylthiobenzylidene analogues. On addition of α-methyl group in sulindac sulfide amide analogues, compound (**80**) and (**81**) did not reflect any improvement showing in *M. tuberculosis* H37Rv and BJ cell data (Fig. 19). But N, N'-dimethylaminoethyl acetamide derivative of Sulindac sulfide with α-methyl (**81**) showed a 4-fold increase in activity than compound (**69**) and N, *N*-dimethylaminoethyl analogues (**80**) was 2-fold less active than its desmethyl analogue (**67**).

Further Sulindac sulfide amide derivatives were extended to prepare compounds (**82**, **83**) from compound **69** by linking with L-valine (Fig. 20). The inhibitory activity of α-methyl analogue **83** demonstrated six-fold more active than its desmethyl analogue **56** against H37Rv.

The inactive compounds (**72**) and (**74**) activity can be enhanced by analogues exploring the amine linkage at the C-3 position (compound **84, 85** and **86**) (Fig. 21). The compound (**60**) with piperidinylethyl analogues showed 6-fold more activity than its corresponding amide analogue (**70**). The activity of E-conformation of sulindac analogues (**87**) to (**89**) was tested against whole bacteria and *Mtb* FtsZ (Fig. 22). But it was found to show that there is no significant difference between the E and Z forms of the compounds (**67**) and (**87**) (see Fig. 23).

The Mtb FtsZ Polymerization, Tubulin Polymerization, IC 90 and MIC_{99} of *M. tuberculosis* H37Ra and Rv data of selected Sulindac derivatives were displayed in Table 7. Considering versatile potencies, sulindac analogues remain the most attractive and promising scaffold to develop new FtsZ inhibitors against *M. tuberculosis*.

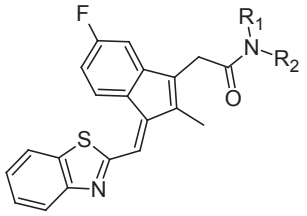

Compounds	R1	R2	MtbH$_{37}$Rv IC90 (μM)
(75)	H	-CH_2CH_2-N(CH_3)$_2$	4.75±0.05
(76)	CH3	-CH_2CH_2-N(CH_3)$_2$	9.97±0.33
(77)	H	-CH_2CH_2-N(CH_2CH_3)$_2$	3.47±0.04
(78)	H	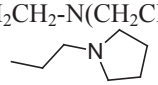	6.70±0.04
(79)	H	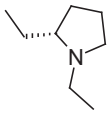	5.46±0.12

Fig. 18. *M. tuberculosis* H37Rv cytotoxicity data of compound (**75**) to (**79**).

3.2.7. Vanillin derivatives

In an effort to search for novel derivatives of vanillin, Sun and co-workers designed, synthesized and evaluated their biological activities as potent FtsZ inhibitor [106]. Among the synthesis twenty vanillin analogues, compound **98** demonstrated the highest antibacterial activity with a MIC of 0.28 μg/ml against *E. coli* strains as compared to *B. subtilis*, *P. aeruginosa*, and *S. aureus* strain (Fig. 23 and Table 8). The antibacterial activity vanillin derivatives were found to less with the introduction of two chlorine groups in the benzene ring (31.02–45.67 μg/ml). Based on the activity data it is shown that electron-donating groups on benzoic acid component were favorable for activity and compounds with electron-with-drawing halogen groups on benzoic acid component were not exhibited for potency. It also exerted the best potency of FtsZ inhibitory activity with polymerization IC50 of 2.1 μM done by the light-scattering assay. Other tested compounds displayed moderate inhibitory activities with IC50 ranging from 9.4 to 85.8 μM. The potency of this structural composition of compound **98** was also confirmed via docking studies and found to show the lowest internal energy. Docking studies showed the compound **98** interacted with FtsZ protein complex structure (PDB ID 2VAM) by means of hydrogen bonds at Asp 46, Ala 73, Gly 108, Arg 143 and π-cation interactions existed between the benzene ring and amino acids Arg 143. The potency of vanillin analogues may be exploited in future studies for the development of FtsZ-targeted antibacterial agents.

3.2.8. Isoquinoline derivatives

As the presence of hydrophobic functionality identified in both the structure of sanguinarine and berberine to strengthen the antibacterial activity, Kelley et al. further extend their work in simplification way to design new compounds representing each with the core structure of 3-phenyl isoquinoline [107,108]. Eventually, 3-phenylisoquinolines and 3-phenylisoquinolinium derivatives were synthesized and evaluated for their antibacterial activity against *S. aureus* and *E. faecalis*, including multidrug-resistant strains of methicillin-resistant *S. aureus* (MRSA) and vancomycin-resistant *E. faecalis* (VRE). The activity was noticed to be significant for quaternary isoquinoline derivatives and potency of antibacterial activity enhanced with the increased lipophilicity of the substituent at the 3′-position. The experimental studies reveal that several 3-phenylisoquinolinium derivatives such as **(103)** to **(105)**, **(106)**, and **(108)** have MIC values that range from 2 to 4 μg/ml against MSSA and MRSA (Fig. 24). The compounds **(103)** and **(105)** each exhibited MIC value of 8 μg/ml against VRE. The more lipophilic compounds, such as 3-(3′-biphenyl) isoquinoline or 3-3′-terphenyl) isoquinoline, exhibited greater antibacterial activity. Most of the quaternary ammonium derivatives, **(99)** and **(100)** had MICs of 1 μg/ml against MSSA and 1–8 μg/ml against MRSA (Fig. 24).

However, the derivatives of these 6, 7-dimethoxyisoquinoline compounds and **(102)** was found to be more toxic with an IC50 value of 3.5 μM in MDCK cells using the MTT-microtiter plate tetrazolinium cytotoxicity assay. The synthesized isoquinolene derivative, compounds (**99**, **100**, **102**, **104**, **105**, **106** and **107**) inhibit the GTPase activity of SaFtsZ by as much as 85%, which was assayed by measuring the inorganic phosphate (*Pi*) released upon GTP hydrolysis by malachite green colorimetric assay. At a concentration of 40 μg/ml, the active isoquinoline compounds **99**, **100**, **102**, **104**, **105**, **106** and **107** were found to stimulate *Sa* FtsZ polymerization with MIC values ≤ 16 μg/ml,

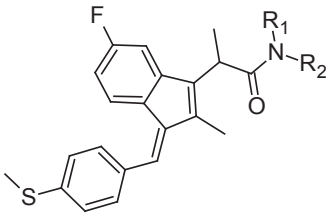

Compounds	R1	R2	*Mtb*H$_{37}$Rv IC90 (μM)
(80)	H	-$CH_2CH_2N(CH_3)_2$	13.58±0.89
(81)	CH3	-CH_2CH_2NH-CH_3	2.11±0.08

Fig. 19. *M. tuberculosis* H37Rv activity of the compound (80) and (81).

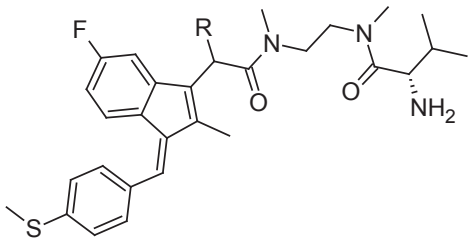

Compounds	R	*Mtb*H_{37}Rv IC90 (μM)
(82)	H	4.34±0.06
(83)	CH3	0.74±0.01

Fig. 20. *M. tuberculosis* H37Rv activity of the compound (**82**) and (**83**).

monitored by using a microtiter plate-based light scattering (turbidity) assay at 340 nm absorbance. Furthermore, Toxicological assessment of isoquinoline compounds revealed minimal cross-reaction mammalian β- tubulin as well as little or no human cytotoxicity. An effort towards the successfully structural simplification of natural products and antibacterial activity accelerated the discovery and development of 6, 7-dimethoxyisoquinoline derivatives as novel nontoxic FtsZ inhibitors.

3.2.9. DAPI

Widening the spectacular work on tubulin, Nova et al. studied 4′,6-diamidino-2-phenylindole **(109)** (Fig. 25), as a fluorescence probe has high binding affinity located on the main body (tubulin S), protected by C-terminal region and characterized interaction of DAPI with *E. coli* FtsZ [109]. On binding, it was found to show bundling of FtsZ protofilament, causing inhibition of GTPase activity. The GTPase assay proved that DAPI acted as a noncompetitive inhibitor of *E. coli* FtsZ with a Ki of 29.4 ± 0.3 μM. The fluorescence anisotropy was measured in the titration of DAPI, giving the dissociation constant with a value of 16.6 mM, suggesting the activity of bundling of the protofilament and the inhibition of GTPase activity. These results assist the inhibitory effect of DAPI on the *E. coli* FtsZ GTPase activity which in turn are responsible for the stability of the polymer during the polymerization process and hence can be used in drug development strategy as an antibacterial agent.

3.2.10. OTBA

On screening from 81 different compounds, Beuria et al was found to identify a rhodanine class of compound, OTBA (3-{5-[4-oxo-2-thioxo-3-(3-trifluoromethylphenyl)- thiazolidin-5-ylidenemethyl]-furan-2-yl}-benzoic acid) **(110)** (Fig. 25) has been assisted to disturb the formation and function of the Z-ring via altering FtsZ assembly dynamics [110]. OTBA bound to FtsZ with an apparent dissociation constant of 15 ± 1.5 μM. The effects of light scattering on *Ec*FtsZ was enhanced by approx. 3-fold in the presence of 25 μM OTBA, suggesting increased bundling of FtsZ protofilaments. Moreover, OTBA was found to inhibit the growth of *B. subtilis* 168 cells with a MIC of 2 μM which evincing its potency as an antibacterial drug. As compared to *B. subtilis cell,* OTBA has a weak inhibitory effect on the proliferation of *E. coli* cells by finding increase the length of *E. coli* cells. Beuria et al. also have compared the mechanism of action of OTBA with the most of anticancer agent paclitaxel (Taxol), which finds in the mode of mammalian cell proliferation via stabilization of microtubules, thereby disturbing the mitotic spindle assembly [111]. Thus OTBA can be commended as a favorable FtsZ-targeting antibacterial agent with lower toxicity.

3.2.11. Trisubstituted benzimidazoles

Visualizing the structural similarity and involving with anti-FtsZ activity of the pyridopyrazine moiety, pteridine moiety, albendazole, and thiabendazole, Kumar et al. designed and synthesized a library of novel molecules with benzimidazole scaffold through rational drug design [112]. The newly developed synthesized libraries of 2,5,6- and 2,5,7-trisubstituted benzimidazoles (349 compounds) were screened for their activity against MtbH37Rv using the “Microplate Alamar Blue assay (MABA)” (Fig. 26) [113]. Among them, some of the benzimidazoles exhibited promising MIC values in the range of 0.5–6 μg/ml (2–15 μM) for their antibacterial activity against *M. tuberculosis* H37Rv strain. Besides five of the lead compounds **(111)**, **(112)**, **(113)**, **(114)**, and **(115)** displayed excellent activity against the drug-resistant strains

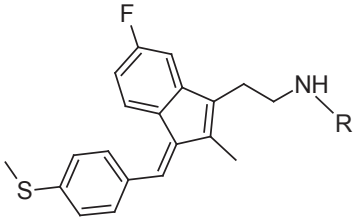

Compounds	R	*Mtb*H_{37}Rv IC90 (μM)
(84)	benzyl	2.07±0.01
(85)	Furan-2-ylmethyl	1.69±0.06
(86)	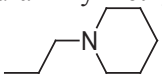	0.88±0.01

Fig. 21. *M. tuberculosis* H37Rv activity of the compound (**84**) to (**86**).

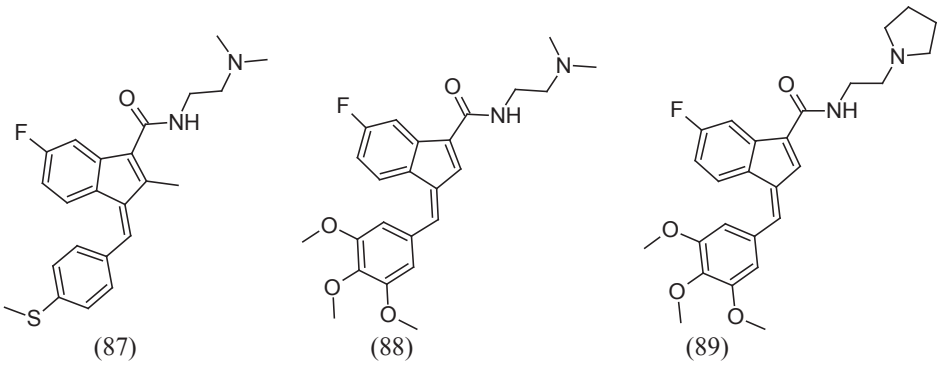

Compounds	*Mtb*H_{37}Rv IC90 (μM)
(87)	7.7±0.33
(88)	>100*
(89)	25.48±0.33

*82% inhibitions at 50μM

Fig. 22. *M. tuberculosis* H37Rv activity of sulindac three E-conformers.

to that against the *M. tuberculosis* H37Rv, shown in Table 9. Fortunately, FtsZ polymerization by light scattering assay evaluated the lead compounds inhibited FtsZ assembly in a dose-dependent manner and do not show appreciable cytotoxicity effect (IC50 > 200 μM) against Vero cells. The lead compounds **(111)** and **(112)** showed unpredicted enhancement of the GTPase activity of *Mtb* FtsZ, indicating impaired in FtsZ assembly and leading to efficient inhibition of FtsZ polymerization and filament formation. In addition Transmission Electron Microscopy (TEM) and SEM analyses strongly intimated that lead benzimidazoles have a novel mechanism of action on the inhibition of *Mtb* FtsZ assembly and Z-ring formation (see Fig. 26).

The comprehensive SAR study on 2-cyclohexyl-5, 6-disubstituted benzimidazoles was performed to optimize the nitrogen substituents at the 5 and 6 positions of these two lead compounds **(112)** and **(113)** through systematic modifications [114]. As the 6-amino group exerts distinctive antibacterial effects, a small dimethylamino group in compound **116** at this position dramatically increases the potency as compared to long or bulky 6-alkylamino groups. The advance in the development of early lead compound finding in this SAR study has assisted to the introduction of **(116)** with exceptional potency (MIC 0.06 μg/ml) against *M. tuberculosis* H37Rv strain, which supports a butoxy carbonyl amino group at the 5th position and a dimethylamino group at the 6th position. The TEM analysis demonstrated that **(116)** not only significantly reduced the density and population of FtsZ polymers, protofilaments, and aggregates, but also apparently disrupted the formed FtsZ polymers and aggregates. All the results together suggested that the advanced lead benzimidazoles have a novel mechanism

Table 7
Mtb FtsZ, tubulin and *M. tuberculosis* H37Ra and Rv data of sulindac analogues.

Compounds	*Mtb*FtsZ Polymerization IC50(μM)	Tubulin Polymerization IC50(μM)	*M. tuberculosis* H37Rv IC90 (μM)	*Mtb*H37Ra MIC_{99}(μM)
(67)	39.4 ± 4.9	NA	7.29 ± 0.23	8
(69)	34.9 ± 7.0	NA	8.28 ± 0.33	8
(70)	26.5 ± 4.8	NA	1.41 ± 0.03	> 4 ≤ 64
(73)	22.9 ± 4.8	NA	> 100*	64
(82)	38.0 ± 6.3	NA	4.34 ± 0.06	8
(87)	44.6 ± 6.3	NA	7.70 ± 0.33	16
(88)	43.3 ± 9.8	NA	> 100	32
(89)	37.6 ± 5.7	NA	25.48 ± 0.33	32

NA = Not active up to 100 μM.
* 82% inhibitions at 50 μM.

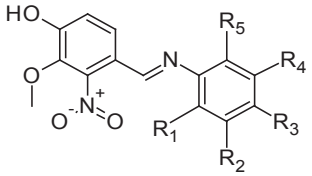

Compounds	R_1	R_2	R_3	R_4	R_5
(90)	H	Cl	Cl	H	H
(91)	Cl	H	Cl	H	H
(92)	Cl	H	H	Cl	H
(93)	CH_3	H	H	CH_3	H
(94)	H	CH_3	CH_3	H	H
(95	CH_3	H	H	H	CH_3
(96)	CH_3	H	H	H	CH_3
(97)	NO_2	H	Cl	H	H
(98)	$(CH_3)_2CH_2$	H	H	H	$(CH_3)_2CH_2$

Fig. 23. Structures of Vanillin analogues.

Table 8
Antibacterial and FtsZ inhibitory activity of compounds.

Compounds	MIC (μg/ml)				
	E. coli ATCC35218	*P. aeruginosa* ATCC13525	*B. subtilis* ATCC6633	*S. aureus* ATCC6538	Polymerization IC50 (μM)
(**90**)	41.11	37.56	33.92	38.99	85.80
(**91**)	32.18	38.92	41	45.67	77.64
(**92**)	31.02	38.64	41.33	45.01	72.13
(**93**)	3.45	5.12	21.58	17.19	15.47
(**94**)	21.59	20.83	2.78	6.92	22.98
(**95**)	6.12	5.02	2.89	11.34	9.4
(**96**)	18.46	15.11	20.1	26.95	41.01
(**97**)	31.20	28.47	33.89	37.82	50.11
(**98**)	**0.28**	**5.89**	**3.31**	**2.03**	**2.1**

of action on the inhibition of *Mtb* FtsZ assembly and Z-ring formation.

In a continued effort to find effective compounds against FtsZ, Knudson et al. designed and synthesized a new series of trisubstituted benzimidazoles based on SAR studies on previously reported selected benzimidazoles demonstrated activity against *M. tuberculosis* H37Rv [115]. The expansion of work reported the currently developed lead compound, **(117)** from several 2-cyclohexyl-5-acylamino-6-N, *N*-dimethyl amino benzimidazoles. The MIC for **(117)** against different clinical strains of *M. tuberculosis* was 0.16 μg/ml. Compound **(117)** demonstrated the ability of the compound to inhibit polymerization and aggregation. Transmission electron microscopy (TEM) imaging of *Mtb* FtsZ indicated that at 80 μM, the effect was more apparent with the

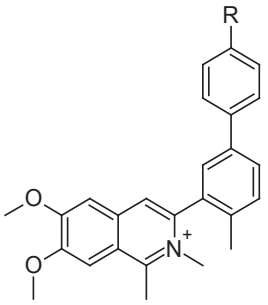

(99): R= phenyl, (100): R= t-butyl

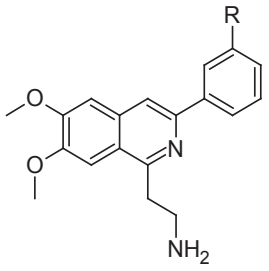

(101): R= phenyl, (102): R= t-butyl

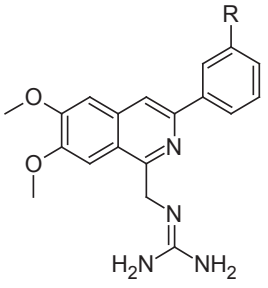

(103): R= phenyl, (104): R= t-butyl

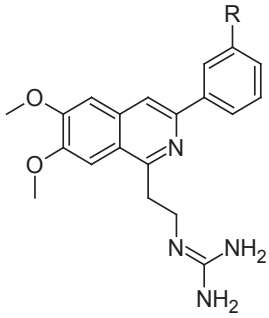

(105): R= phenyl, (106): R= t-butyl

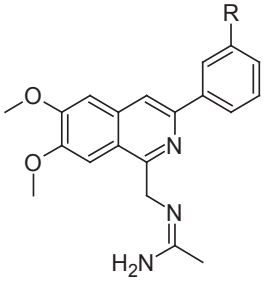

(107): R= t-butyl

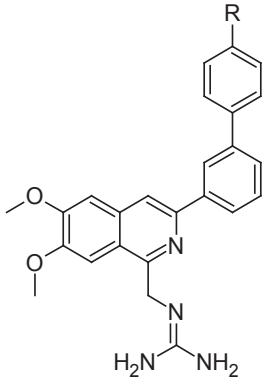

(108): R= t-butyl

Fig. 24. Structure of isoquinolene derivative.

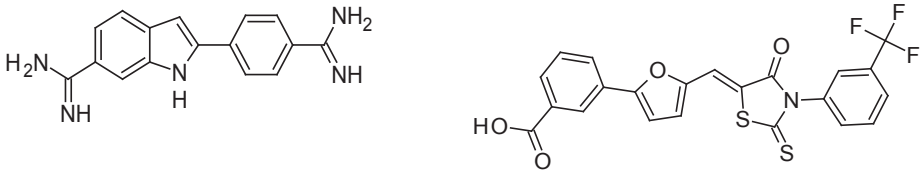

DAPI (109) OTBA(110)

Fig. 25. Structure of compound (**109**) and (**110**).

dispersion of the FtsZ polymer. The activity of **(117)** was determined to be concentration-dependent and to have excellent stability in mouse and human plasma, and liver microsomes. This study has given the way for the further optimization of trisubstituted benzimidazoles and continue to be a platform for the development of novel inhibitors with efficacy.

To further explore the effect of substituents other than amines at the 6-position on antibacterial activity, Park et al. designed and synthesized a new series of 2, 5, 6-trisubstituted benzimidazole library with ether/thioether groups at the 6-position [116]. All the newly synthetic compounds screened against drug-sensitive *M. tuberculosis* H37Rv strain using the "Microplate Alamar Blue Assay (MABA). Of these hits, compound **(118),** bearing *n*-butoxycarbonylamino group at the 5th position gave the best potency MIC 0.63 μg/ml) against *M. tuberculosis* H37Rv. FtsZ polymerization by Light scattering assay and TEM analysis with the most potent compound **(118)** clearly indicate that the two selected compounds inhibit FtsZ assembly in a dose-dependent manner. The dissociation constant (K_d) of **(118)** was determined to be 1.32 μM based on its fluorescent anisotropy which imparted direct evidence for the binding interaction between this benzimidazole and *Mtb*-FtsZ protein. This study strongly supported the importance of compounds, bearing a 4-fluorophenoxy group at the 6th position, a carbamate group at the 5th position for its better activity. These results are quite impressive by taking the compound **118** as *Mtb* FtsZ target for its antibacterial activity and further biological evolution against various other pathogens will be carried out to investigate its pathogen-specific as well as broad-spectrum antibacterial activities.

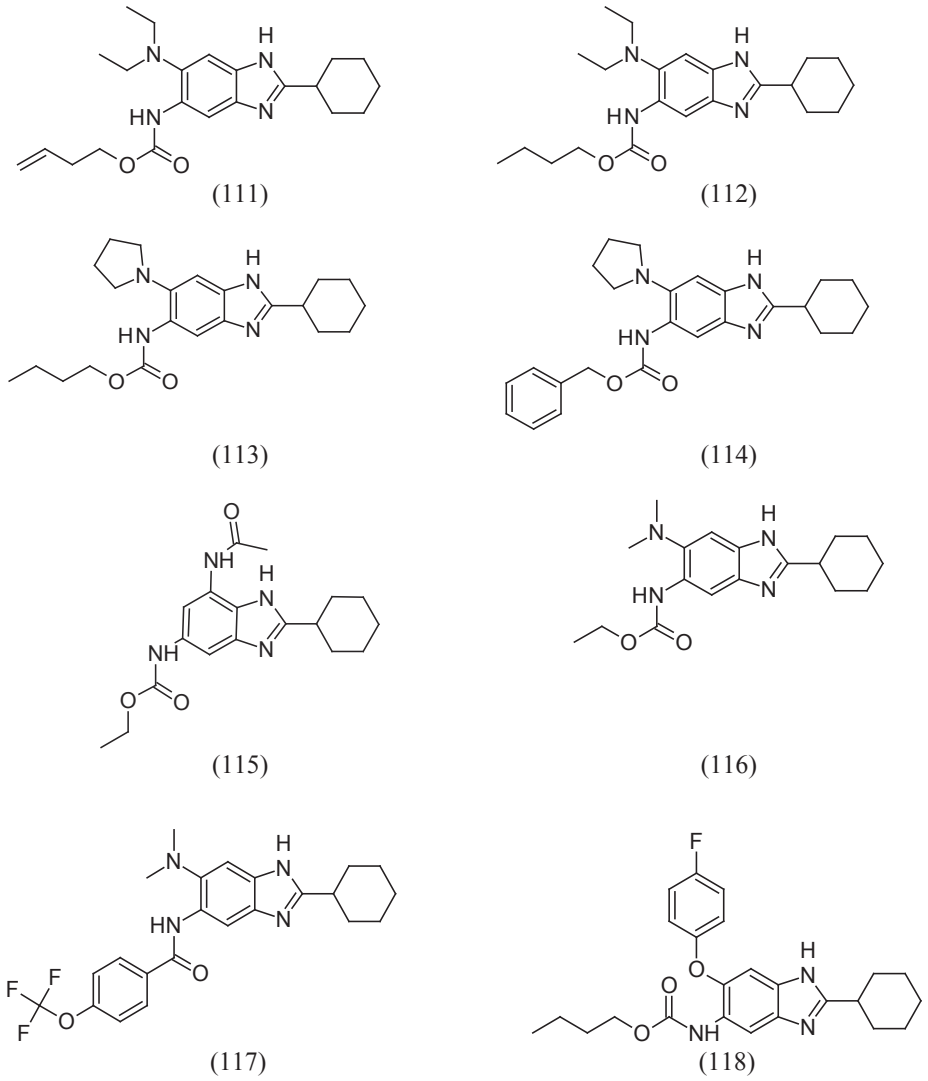

Fig. 26. Structure of trisubstituted benzimidazoles.

Table 9
Compounds on the GTPase activity of *Sa* FtsZ.

Compounds	% GTPase activity
(**99**)	30.2 ± 0.3
(**100**)	14.9 ± 1.7
(**102**)	59.7 ± 1.0
(**105**)	56.0 ± 1.7
(**107**)	64.8 ± 0.1
(**104**)	60.4 ± 1.9

3.2.12. Arene-diol digallates

In order to search for non-nucleotide inhibitors that could replace the nucleotide in FtsZ, Ruiz-Avila et al. to screens selective compounds from the literature, virtual screening (VS) hits, and in-house compounds [117]. The collected compounds were screened by docking into *Bs* FtsZ GTP binding site and further employed the mant-GTP anisotropy method adapted to bind bacterial *Bs* FtsZ. Compounds from the in-house library after docking into the *Bs* FtsZ GTP site found that several polyhydroxy derivatives that competitively displace mant-GTP from Bs-FtsZ. Compound UCM05 **(119)** and its fragments UCM16 **(120)** and UCM17 **(121)** showed significant affinity to *Bs*-FtsZ. Further Compound UCM05 **(119)** and its analogues UCM44 **(122)**, 25 μM; UCM53 **(123)** were identified to inhibit the growth of the Gram-positive bacterium *B. subtilis* with MIC values of 100 μM, 25 μM, and 13 μM, respectively but lack activity on the Gram-negative bacterium *E. coli* (Fig. 27). The polyhydroxy aromatic compound UCM05 **(119)** and its simplified analogue UCM44 **(122)** that specifically bind to *B. subtilis* FtsZ monomers with micromolar affinities and perturb normal assembly, as studied with light scattering, polymer sedimentation, and negative stain electron microscopy. The GTPase assay showed a weak (20%) inhibition of both compounds UCM05 **(119)** and UCM44 **(122)** against the GTPase activity. The docking study suggested that the phenolic groups and the naphthalene core of UCM05 **(119)** and UCM44 **(122)** occupied the phosphate and nucleic base binding sites of GTP and hence selectively inhibited FtsZ. The compounds UCM05 **(119)**, UCM44 **(122)**, and UCM53 **(123)** were inhibited cell division by inducing filamentation of *B. subtilis* cells, showing a phenotypic response of FtsZ inhibition. These three compounds induced numerous punctuate foci and distorted ring structures in *B. subtilis* SU570 cells by employing fused FtsZ-GFP to visualize the Z ring. However these compounds inhibit mammalian cells growth at concentrations partially overlapping the bacterial MICs and among them, UCM53 **(123)** displayed the best selectivity [IC50 (HeLa)/MIC (*S. aureus* MR 12160636) = 5].

Starting from inhibitors UCM05 **(119)** and UCM44 **(122)**, a series of small molecule inhibitors were synthesized and analyzed for their potencies. These newly synthesized inhibitors interact with the GTP-binding site with a K_d value of 0.4–0.8 μM and display antibacterial activity against Gram-positive pathogenic bacteria. The lead compounds play as an effective FtsZ assembly modifier and lead to filamentous undivided cells, finally disrupting bacterial Cell division. Among the series of biphenyl derivative, compound **124** acts as a potent FtsZ inhibitor with a K_d value of 0.5 μM and high antibacterial activity [MIC = 7 μM] against MRSA (Fig. 27) [118].

3.2.13. Taxane

Taxane was screened to represent highly cytotoxic taxoids that stabilize microtubules and noncytotoxic (or very weakly cytotoxic) taxane-multidrug-resistance (MDR) reversal agents (TRAs) that inhibit the efflux pumps of ATP-binding cassette (ABC) transporters such as P-glycoprotein. Huang et al. reported the screening of 120 taxanes that exhibited significant antituberculosis activity [119]. The selected compounds on rational optimization led to the discovery that the C-seco-taxane multidrug-resistance (MDR) reversal agents (C seco-TRAs) are noncytotoxic. So, C-seco-baccatin analogues of SB-RA-2001 (**125**), SB-RA-5001 (**127**), and its congeners were synthesized and evaluated (Fig. 28). Structure of. It was found that C-seco-TRA stabilizes FtsZ protofilaments of *M. tuberculosis* cells in a light-scattering assay, which was similar to paclitaxel as an anticancer agent that promotes tubulin assembly and stabilizes microtubules. These noncytotoxic taxane lead compounds exhibited MIC_{99} values of 1.25 to 2.5 μM against drug-resistant and drug-sensitive strains of *M. tuberculosis*. The treatment of

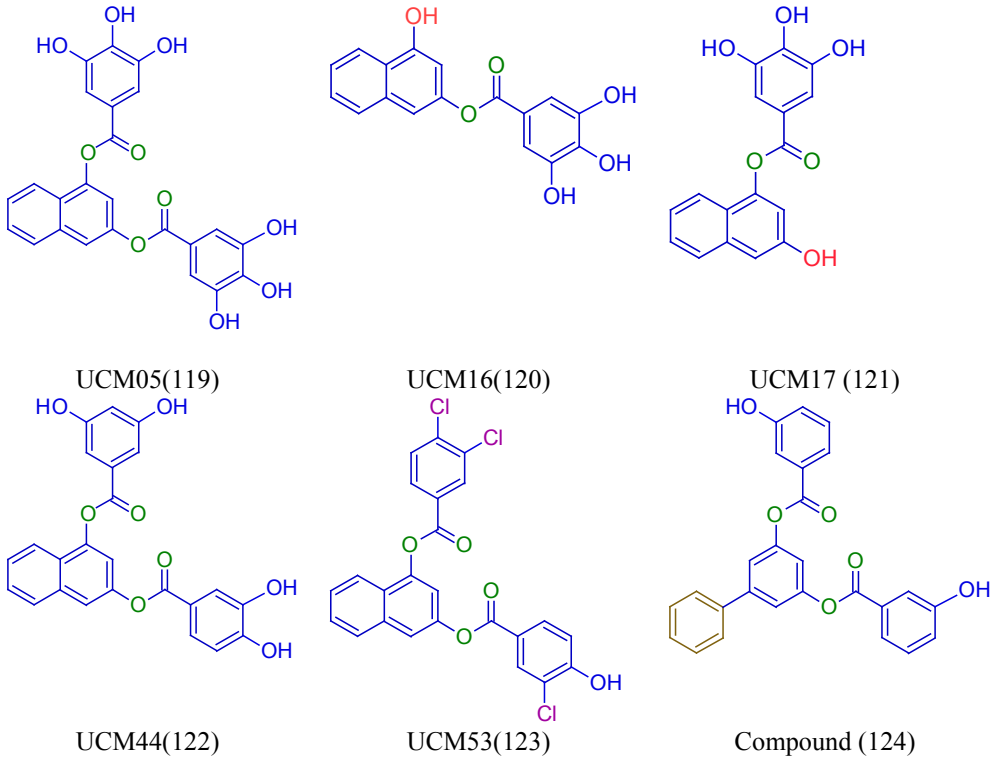

Fig. 27. Structure of Arene-diol digallates.

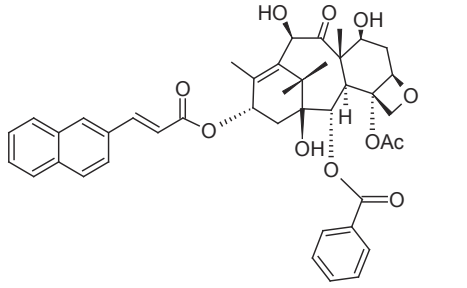

SB-RA2001(125)

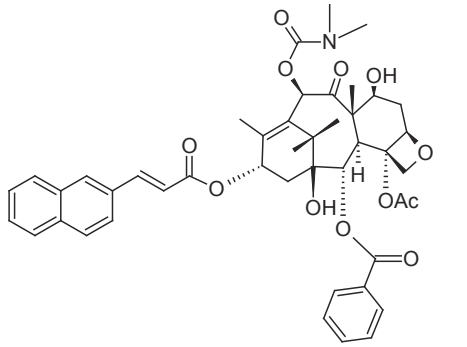

SB-RA2018(126)

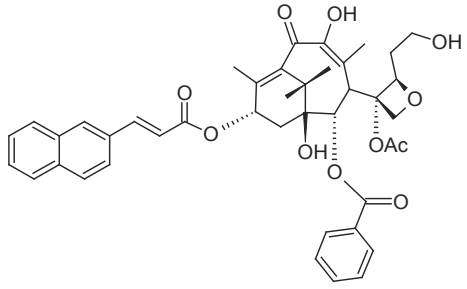

SB-RA5001(127)

Fig. 28. Structure of Taxanes.

Mtb cells with SB-RA-2018 (**126**) and SB-RA-5001 based on scanning electron microscopy (SEM) analysis showed filamentation and prolongation of the cells, a phenotypic response to FtsZ inactivation. The observation of Transition electron microscopy (TEM) analysis of *Mtb* FtsZ with SB-RA-5001 (**127**) indicated that it stabilized *Mtb* FtsZ polymers (see Fig. 28).

Singh et al reported that a taxane SB-RA-2001 inhibited the proliferation of *B. subtilis* 168 and *M. smegmatis* cells with minimal inhibitory concentrations of 38 and 60 μM, respectively [120]. SB-RA-2001 effectively inhibited the proliferation of bacterial cells by perturbing the formation of the Z-ring in *B. subtilis* 168 cells without disturbing nucleoid segregation, indicating FtsZ as the target. In vitro, SB-RA-2001 bound to FtsZ with modest affinity stimulated the assembly and bundling of FtsZ protofilaments and reduced the GTPase activity of FtsZ. The computational study suggested that SB-RA-2001 binds to FtsZ in the cleft region between the C-terminal domain and helix H, and its binding to FtsZ resembled that of PC190723. The resultant activity of SB-RA-2001 and SB-RA-5001 together suggest that it would consider as lead molecules and that further modification of their structures could help in the development of potent taxane-based FtsZ-inhibitors.

3.3. Others

MciZ is a 40-amino acid peptide that acts during sporulation to block Z-ring formation in the mother cell and act by inhibiting the polymerization of, FtsZ. Handler et al. investigated the effect of MciZ on Z-ring formation in *B. subtilis* [121]. MciZ binds to FtsZ by affinity chromatography using His-tagged FtsZ caused the retention of MciZ. It is seen that at low and intermediate concentrations of GTP, inhibition of polymerization of MciZ was highly effective. During sporulation, MciZ was produced under the control of the transcription factor σ^E. The absence of MciZ develops Z-ring in the mother-cell compartment of *mciZ* mutant sporangia when cytokinetic events normally have ceased the ring.

A murine defense peptide-like Cathelin-related antimicrobial peptide (CRAMP), peptide-based FtsZ-inhibitors with 37 amino acid residues that supports the immune system by binding to bacterial cell surfaces [122]. It showed MIC values ranging from 0.5 μM to 64 μM against various strains of bacteria, such as *E. coli,* MRSA*, B. megaterium* and *S. typhimurium*. CRAMP exhibited a dose-dependent inhibition of FtsZ polymerization by Light scattering analysis of FtsZ, while tubulin polymerization was unaffected. The polymerization of CRAMP was ruptured by binding of FtsZ near the T7 loop and distorted the monomer-monomer interaction of FtsZ.

Shimotohno et al identified a polypeptide antibiotic, edeine obtained from *Bacillus brevis* found to inhibit Z-ring formation [123]. Edeine exists in two forms, edeine A and edeine B, which differ in the base moiety and further differentiated into two reversible isomers like edeine A1, A2, and edeine B1, B2, respectively. The isomers of edeine A1 and edeine B1 are active while other two isomers of edeine A2 and edeine B2 are inactive. The active isomer Edeine A1 inhibits DNA and protein synthesis within bacteria, emerging in a filamentous phenotype.

Peptide nucleic acids (PNAs) are oligonucleotide analogues with a polypeptide-like backbone instead of a ribose-phosphate backbone [124]. Based on the best result from dot-blot hybridization, a PNA oligomer was synthesized and conjugated to the cell penetrating peptide, (RXR)4XB, for improved internalization into cells. The first conjugate, PPNA1, was complementary to nucleotides 309–323 of ftsZ-mRNA and the second conjugate, PPNA2, was synthesized from the translation initiation and ribosome binding sites of FtsZ-mRNA. Both the conjugates inhibited the growth of MRSA CY-11 strain in a dose-dependent manner and showed complete growth inhibition at 30 μM for PPNA1 and 40 μM for PPNA2 [125]. Cell viability assays indicated that only PPNA1 acted as bactericidal at 40 μM of both compounds.

Locked nucleic acids (LNA) are nucleic acid analogues with the ribose ring locked by a 2′-O, 4′-C-methylene bridge and its oligomeric chains have high affinity to complementary strands of RNA or DNA, act by silencing target genes [126]. The LNA portion of peptide LNA787 was complementary to the nucleotides 787–808 fragment of MRSA ftsZ-mRNA and its cell-penetrating peptide, (KFF) 3 K on conjugation with ten strains of *S. aureus* with MIC values of 1.56 to 12.5 μM. Peptide LNA787 was intimated to inhibit cell division in various MRSA strains by silencing the ftsZ gene and intercepting protein expression.

4. Conclusion and future prospects

Bacterial cytokinesis FtsZ protein is a promising molecular target for new generation antibacterial drug discovery. This review has covered the information on a different group of natural products as well as synthetic small molecules, targeting FtsZ that are effective against various pathogens, including *S. aureus,* methicillin-sensitive *S. aureus,* methicillin-resistant *S. aureus, E. coli, VRE, B. subtilis*, *M. tuberculosis,* etc. Some of the identified FtsZ inhibitors include natural products such as berberine, viriditoxin, totarol, and synthetic compounds like PC190723, SRI3072, and OTBA. These molecules show potent activity by inhibiting the action of polymerization and GTPase activity. Though FtsZ is homologous to eukaryotic cytoskeleton protein tubulin, the study of these inhibitors exhibited their potency without any effects on tubulin assembly.

Simplification and structural modification of natural product-based FtsZ inhibitors like cinnamaldehyde, totarrol, coumarin, sanguinarine,

berberine, phenylpropanoids on, has fabricated a series of compounds with MIC value in the range of μg/mL. The antibacterial activity was specifically found to be effective through compounds like cinnamaldehyde, phenylpropanoids and their derivatives containing reactive α, β-unsaturated carbonyl moiety of chalcones. The advanced technology in target validation assay and well methods of screening procedure would facilitate the introduction of novel FtsZ inhibitors from natural sources. As described here, several FtsZ inhibitors identified were found to be highly promising candidates for the further preclinical investigation. Among them, a benzamide based small molecule, PC190723 exhibits potent bactericidal activity against various staphylococcal strains. The clinical development of prodrugs of PC190723 (e.g. TXA-709 and TXA-707) resulted in increased pharmaceutical properties, which, in turn, led to improved intravenous as well as in vivo oral efficacy against both MSSA and MRSA. Owing to their efficient antibacterial properties, minimum cytotoxicity to mammalian tissues and improved pharmacokinetic properties, there are chances for TXA709 to enter the market as a prime FtsZ inhibitor against the staphylococcal infections in the near future. Besides most of the promising FtsZ inhibitors like OTBA, taxanes, derivatives of sulindac, trisubstituted benzimidazoles were found to inhibit GTPase activity/polymerization/nucleation of *M. tuberculosis* and were considered as a platform of antitubercular drugs for preclinical drug development.

Since several classes of FtsZ inhibitors have been investigated to acquire antibacterial properties, no inhibitor has stepped ahead for clinical trial as yet. Limited crystal structure data of FtsZ has influenced the insufficient structural information to design potent inhibitors. Even though more than 30 crystal structures have been deposited in Protein Data Bank, only 30% of them are found as *S. aureus* FtsZ co-complex with PC 190723 [127]. Additional structural biology data about the binding interaction of FtsZ bound protein and inhibitors could contribute a detailed insight into the design of inhibitors. To summarize, the demand, interest, and experience in the field of research on FtsZ has established a promising molecular target for the design of potent antibacterial agents. Ongoing systematic research with advanced experimental techniques and *in silico* computational studies should encourage the discovery of FtsZ inhibitors as a new generation of antibacterial agents.

Declaration of Competing Interest

The authors declare no conflict of interest.

Acknowledgements

We would like to thank Dr. Manal Mohammed, Associate Professor, Department of Pharmaceutical Chemistry, KTN College of Pharmacy, Puliyanamkunnu, Kerala, India for proof reading this article.

Grant Information

It is to be mentioned with thank and gratitude for the Grant received by Swayansiddha Tripathy, from Department of Science and Technology Ministry of Science and Technology, Government of India, New Delhi, India, for the financial support under Women Scientist Scheme, WOS-A (file number No. SR/WOS-A/CS-1108/2015-G).

References

[1] E.F. Bi, J. Lutkenhaus, J. Bacteriol. 172 (1990) 2765–2768 PubMed: 2158979.
[2] G. Tan, M. Chen, C. Foote, C. Tan, Genetics 183 (1) (2009) 13–22, https://doi.org/10.1534/genetics.109.104794.
[3] B. Beall, J. Lutkenhaus, Genes & Dev. 5 (1991) 447–455, https://doi.org/10.1101/gad.5.3.447.
[4] K. Dai, J. Lutkenhaus, J. Bacteriol. 173 (11) (1991) 3500–3506 PMID: 2045370.
[5] M.G. Pinho, J. Errington, Mol. Microbiol. 50 (3) (2003) 871–881 PMID:14617148.
[6] A.F. Chalker, R.D. Lunsford, Pharmacol Ther. 95 (1) (2002) 1–20 PMID: 12163125.
[7] H.P. Erickson, Trends Cell Biol. 8 (4) (1998) 133–137 PMID: 9695825.
[8] J. Lowe, F. Van den Ent, L.A. Amos, Annu. Rev. Biophys. Biomol. Struct. 33 (2004) 177–198, https://doi.org/10.1146/annurev.biophys.33.110502.132647.
[9] K.A. Michie, J. Lowe, Annu. Rev. Biochem. 75 (2006) 467–492, https://doi.org/10.1146/annurev.biochem.75.103004.142452.
[10] L. Mosyak, Y. Zhang, E. Glasfeld, S. Haney, M. Stahl, J. Seehra, W.S. Somers, EMBO J. 19 (13) (2000) 3179–3191, https://doi.org/10.1093/emboj/19.13.3179.
[11] K. Yan, K. Pearce, D.J. Payne, Biochem. Biophys. Res. Commun. 270 (2000) 387–392.
[12] W. Margolin, Nat. Rev. Mol. Cell Biol. 6 (11) (2005) 862–871, https://doi.org/10.1038/nrm1745.
[13] M. Loose, T.J. Mitchison, Nat. Cell Biol. 16 (2014) 38–46, https://doi.org/10.1038/ncb2885.
[14] K. Lowe, L.A. Amos, Nature 391 (1998) 203–206, https://doi.org/10.1038/34472.
[15] E. Nogales, K.H. Downing, L.A. Amos, J. Löwe, Nat. Struct. Mol. Biol. 5 (1998) 451–458 PMID: 9628483.
[16] E.F. Bi, J. Lutkenhaus, Nature 354 (6349) (1991) 161–164, https://doi.org/10.1038/354161a0.
[17] P.A. Levin, R. Losick, Genes Dev. 10 (1996) 478–488, https://doi.org/10.1101/gad.10.4.478.
[18] J. Stricker, P. Maddox, E.D. Salmon, H.P. Erickson, Proc. Natl. Acad. Sci USA (2002), https://doi.org/10.1073/pnas.052595099.
[19] G. Fu, T. Huang, J. Buss, C. Coltharp, Z. Hensel, J. Xiao, PLOS ONE 5 (9) (2010) e12680, https://doi.org/10.1371/journal.pone.0012680.
[20] P.C. Jennings, G.C. Cox, L.G. Monahan, E.J. Harry, Micron 42 (4) (2011) 336–341, https://doi.org/10.1016/j.micron.2010.09.003.
[21] C. Lu, M. Reedy, H.P.J. Erickson, Bacteriology 182 (2000) 164–170, https://doi.org/10.1128/JB.182.1.164-170.2000.
[22] R. Jaiswal, D. Panda, Protein Sci. 17 (2008) 846–854, https://doi.org/10.1110/ps.083452008.
[23] J. Errington, R.A. Daniel, D.J. Scheffers, Microbiol. Mol. Biol. Rev. 67 (2003) 52–65, https://doi.org/10.1128/MMBR.67.1.52-65.2003.
[24] E. Bi, K. Dai, S. Subbarao, B. Beall, J. Lutkenhaus, Res. Microbiol. 142 (2–3) (1991) 241–252, https://doi.org/10.1016/0923-2508(91)90037-B.
[25] P.C. Peters, M.D. Migocki, C. Thoni, E.J. Harry, Mol. Microbiol. 64 (2007) 487–499, https://doi.org/10.1111/j.1365-2958.2007.05673.x.
[26] Li Zhuo, J.T. Michael, V.B. Yves, J.J. Grant, EMBO J. 26 (2007) 4694–4708, https://doi.org/10.1038/sj.emboj.7601895.
[27] P. Szwedziak, Q. Wang, T.A.M. Bharat, M. Tsim, J. Löwe, eLife 3 (2014) e04601, https://doi.org/10.7554/eLife.04601.
[28] S. Thanedar, W. Margolin, Curr. Biol. 14 (13) (2004) 1167–1173, https://doi.org/10.1016/j.cub.2004.06.048.
[29] J. Moller-Jensen, J. Lowe, Curr. Opi. Cell Biol. 17 (1) (2005) 75–81, https://doi.org/10.1016/j.ceb.2004.11.002.
[30] D.W. Adams, J. J Errington, Nat. Rev. Microbiol. 7 (2009) 642–653, https://doi.org/10.1038/nrmicro2198.
[31] N.W. Goehring, J. Beckwith, Curr. Biol. 15 (13) (2005) 514–526, https://doi.org/10.1016/j.cub.2005.06.038.
[32] J.K. Singh, R.D. Makde, V. Kumar, D. Panda, J. Biol. Chem. 283 (2008) 31116–31124, https://doi.org/10.1074/jbc.M805910200.
[33] A.K.W. Leung, E. Lucile White, L.J. Ross, R.C. Reynolds, J.A. DeVito, D.W. Borhani, Mol. Biol. 342 (3) (2004) 953–970, https://doi.org/10.1016/j.jmb.2004.07.061.
[34] S.L. Milam, M. Osawa, H.P. Erickson, Biophys. J. 103 (2012) 59–68, https://doi.org/10.1016/j.bpj.2012.05.035.
[35] B. Gullbrand, K. NordstrÖm, Mol. Microbiol. 36 (2000) 1349–1359, https://doi.org/10.1046/j.1365-2958.2000.01949.x.
[36] S. Rueda, M. Vicente, J. Mingorance, J. Bacteriol. 185 (11) (2003) 3344–3351, https://doi.org/10.1128/JB.185.11.3344-3351.2003.
[37] L. Romberg, T.J. Mitchison, Biochemistry 43 (1) (2004) 282–288, https://doi.org/10.1021/bi035465r.
[38] C. Lu, M. Reedy, H.P. Erickson, J. Bacteriol. 182 (1) (2000) 164–170, https://doi.org/10.1128/JB.182.1.164-170.2000.
[39] M.A. Oliva, S.C. Cordell, J. Loewe, Nat. Struct. Mol. Biol. 11 (12) (2004) 1243–1250, https://doi.org/10.1038/nsmb855.
[40] M.A. Oliva, S. Sonia Huecas, J.M. Palacios, J.M. Benito, J.M. Valpuesta, J.M. Andreu, J. Biol. Chem. 278 (35) (2003) 33562–33570, https://doi.org/10.1074/jbc.M303798200.
[41] J.F. Diaz, A. Kralicek, J. Mingorance, J.M. Palacios, M. Vicente, J.M. Andreu, J. Biol. Chem. 276 (20) (2001) 17307–17315, https://doi.org/10.1074/jbc.M010920200.
[42] E.L. White, L.J. Ross, R.C. Reynolds, L.E. Seitz, G.D. Moore, D.W. Borhani, J. Bacteriol. 182 (2000) 4028–4034 PMID: 10869082.
[43] A. Mukherjee, K. Dai, J. Lutkenhaus, Proc. Natl. Acad. Sci. USA 90 (3) (1993) 1053–1057 PMID: 8430073.
[44] J. Mingorance, S. Rueda, P. Gomez-Puertas, A. Valencia, M. Vicente, Mol. Microbiol. 41 (1) (2001) 83–91 PMID: 11454202.
[45] L. Romberg, P.A. Levin, Annu. Rev. Microbiol. 57 (2003) 125–154, https://doi.org/10.1146/annurev.micro.57.012903.074300.
[46] A. Mukherjee, J. Lutkenhaus, EMBO J. 17 (2) (1998) 462–469, https://doi.org/10.1093/emboj/17.2.462.
[47] S.G. Addinall, C. Cao, J. Lutkenhaus, J. Bacteriol. 179 (13) (1997) 4277–4284 PMID: 9209044.
[48] E.J. Harry, K. Pogliano, R. Losick, J. Bacteriol. 177 (12) (1995) 3386–3393 PMID: 7768847.

[49] S.G. Addinall, E. Bi, J. Lutkenhaus, J. Bacteriol. 178 (13) (1996) 3877–3884 PMID: 8682793.
[50] Katherine A. Hurley, Thiago M.A. Santos, Gabriella M. Nepomuceno, Valerie Huynh, Jared T. Shaw, Douglas B. Weibel, J. Med. Chem. 59 (15) (2016) 6975–6998, https://doi.org/10.1021/acs.jmedchem.5b01098.
[51] A. Mukherjee, J. Lutkenhaus, J. Bacteriol. 181 (3) (1999) 823–832 PMID: 9922245.
[52] T.K. Beuria, S.S. Krishnakumar, S. Sahar, N. Singh, K. Gupta, M. Meshram, D. Panda, J. Biol. Chem. 278 (2003) 3735–3741, https://doi.org/10.1074/jbc.M205760200.
[53] T.P. Geladopoulos, T.G. Sotiroudis, A.E. Evangelopoulos, Anal. Biochem. 192 (1) (1991) 112–116 PMID: 1646572.
[54] S. Gupta, S. Chakraborty, A. Poddar, N. Sarkar, K.P. Das, B. Bhattacharyya, Proteins Struct. Funct. Genet. 50 (2003) 283–289.
[55] M. Mayer, B. Meyer, Angew. Chem. Int. Ed. 38 (1999) 1784–1788, https://doi.org/10.1002/(SICI)1521 3773(19990614)38:12<1784::AID-ANIE1784>3.0.CO;2-Q.
[56] P. Mayer, S.G. Thomas, A.B. Kunnumakkara, C. Sundaram, K.B. Harikumar, B. Sung, S.T. Tharakan, K. Misra, I.K. Priyadarsini, K.N. Rajasekharan, B.B. Aggarwal, Biochem. Pharm. 76 (2008) 1590–1611, https://doi.org/10.1016/j.bcp.2008.08.008.
[57] S. Tajbakhsh, K. Mohammadi, I. Deilami, K. Zandi, M. Moradali Fouladvand, E. Elissa Ramedani, G. Asayesh, Afr. J. Biotechnol. 7 (21) (2008) 3832–3835, https://doi.org/10.5897/AJB08.790.
[58] D. Rai, J.K. Singh, N. Roy, D. Panda, Biochem. J. 410 (2008) 147–155, https://doi.org/10.1042/BJ20070891.
[59] S. Kaur, N.H. Modi, D. Panda, N. Roy, Eur. J. Med. Chem. 45 (2010) 4209–4214, https://doi.org/10.1016/j.ejmech.2010.06.015.
[60] P. Domadia, S. Swarup, A. Bhunia, J. Sivaraman, D. Dasgupta, Bio Chem. Pharmacol. 7 (4) (2007) 831–840, https://doi.org/10.1016/j.bcp.2007.06.029.
[61] X. Li, J. Sheng, G. Huang, R. Ma, F. Yin, D. Song, C. Zhao, S. Ma, Eur. J. Med. Chem. 97 (2015) 32–41, https://doi.org/10.1016/j.ejmech.2015.04.048 PubMed: 25938986.
[62] L.G. Kornika, Cell Mol. Biol. 53 (2007) 15.
[63] S. Hemaiswarya, R. Soudaminikkutty, M.L. Narasumani, M. Doble, J. Med. Microbiol. 60 (2011) 1317–1325, https://doi.org/10.1099/jmm.0.030536-0.
[64] J.P. Dzoyem, F.A. Kechia, V. Kuete, A.C. Pieme, C.M. Akak, J.G. Tangmouo, P.J. Lohoue, Nat. Prod. Res. 25 (2011) 741–749, https://doi.org/10.1080/14786419.2010.531392.
[65] V. Kuete, S. Alibert-Franco, K.O. Eyong, B. Ngameni, G.N. Folefoc, J.R. Nguemeving, J.G. Tangmouo, G.W. Fotso, J. Komguem, B.M. Ouahouo, BMC Compl. Alternat. Med. (2011), https://doi.org/10.1186/1472-6882-11-42.
[66] A. Bhattacharya, B. Jindal, P. Singh, A. Datta, D. Panda, FEBS J. 280 (2013) 4585–4599, https://doi.org/10.1111/febs.12429.
[67] C. Kontogiorgis, A. Detsi, D. Hadjipavlou-Litina, Expert Opin. Therap. Patent 22 (2012) 437–454, https://doi.org/10.1517/13543776.2012.678835.
[68] S. Duggirala, R.P. Nankar, S. Rajendran, M. Doble, Appl. Biochem. Biotechnol. 174 (2014) 283–296, https://doi.org/10.1007/s12010-014-1056-2.
[69] C.-C. Chiang, M.-J. Cheng, C.-F. Peng, H.-Y. Huang, I.-S. Chen, Chem. Biodivers. 7 (2010) 1728–1736 PubMed: 20658660.
[70] R. Jaiswal, T.K. Beuria, R. Mohan, S.K. Mahajan, D. Panda, Biochem. 46 (2007) 4211–4220, https://doi.org/10.1021/bi602573e.
[71] M.B. Kim, T.E. O'Brien, J.T. Moore, D.E. Anderson, M.H. Foss, D.B. Weibel, B. James, J.B. Ames, J.T. Shaw, ACS Med. Chem. Lett. 3 (2012) 818–822, https://doi.org/10.1021/ml3001775.
[72] T.K. Beuria, M.K. Santra, D. Panda, Biochem. 44 (50) (2005) 16584–16593 PubMed: 16342949.
[73] J. Wolff, L. Knipling, Biochem. 32 (1993) 13334–13339, https://doi.org/10.1021/bi00211a047.
[74] E.J. Gentry, H.B. Jampani, A. Keshavarz-Shokri, M.D. Morton, D.V. Velde, H. Telikepalli, L.A. Mitscher, R. Shawar, D. Humble, W. Baker, J. Nat. Prod. 61 (1998) 1187–1193, https://doi.org/10.1021/np9701889.
[75] H.H. Yu, K.J. Kim, J.D. Cha, H.K. Kim, Y.E. Lee, N.Y. Choi, Y.O. You, J. Med. Food 8 (2005) 454–461, https://doi.org/10.1089/jmf.2005.8.454.
[76] P.N. Domadia, A. Bhunia, J. Sivaraman, S. Swarup, D. Dasgupta, Berberine targets assembly of *Escherichia coli* cell division protein FtsZ, Biochem. 47 (10) (2008) 3225–3234 PubMed: 18275156.
[77] N. Sun, F.-Y. Chan, Y.-J. Lu, M.A.C. Neves, H.-K. Lui, PLoS ONE 9 (5) (2014) e97514, https://doi.org/10.1371/journal.pone.0097514.
[78] P. Panda, A.C. Taviti, S. Suresh Satpati, M.M. Kar, A. Dixit, T.K. Beuria, Doxorubicin inhibits E. coli division by interacting at a novel site in FtsZ, Biochem. J. 471 (2015) 335–346, https://doi.org/10.1042/BJ20150467.
[79] F.R. Cockerill III, M.A. Wikler, J. Alder, M.N. Dudley, G.M. Eliopoulos, M.J. Ferraro, D.K. Hardy, D.W. Hecht, J.A. Hindler, J.B. Patel, Approved Standard, ninth ed., Clinical and Laboratory Standards Institute, Wayne, 2012 CLSI document M07-A9.
[80] S. Urgaonkar, H.S. La Pierre, I. Meir, H. Lund, D.R. Chaudhuri, J.T. Shaw, Org. Lett. 7 (25) (2005) 5609–5612, https://doi.org/10.1021/ol052269z.
[81] K. Suzuki, K. Nozawa, S. Nakajima, K.-I. Kawai, Chem. Pharm. Bull. 38 (1990) 3180–3181, https://doi.org/10.1248/cpb.38.3180.
[82] J. Wang, A. Galgoci, S. Kodali, K.B. Herath, H. Jayasuriya, K. Dorso, F. Vicente, A. Gonzalez, D. Cully, D. Bramhill, S. Singh, J. Biol. Chem. 278 (45) (2003) 44424–44428, https://doi.org/10.1074/jbc.M307625200.
[83] T. Läppchen, A.F. Hartog, V.A. Pinas, G.J. Koomen, T.D. Blaauwen, Biochem. 44 (2005) 7879–7884, https://doi.org/10.1021/bi047297o.
[84] T. Läppchen, V.A. Pinas, A.F. Hartog, G.J. Koomen, C. Schaffner-Barbero, J.M. Andreu, D. Trambaiolo, J. Lowe, A. Juhem, A.V. Popov, T. den Blaauwen, Chem. Biol. 15 (2008) 189–199, https://doi.org/10.1016/j.chembiol.2007.12.013.
[85] S. Huecas, C. Schaffner-Barbero, W. Garcia, H. Yebenes, J.M. Palacios, J.F. Diaz, M. Menendez, J.M. Andreu, J. Biol. Chem. 282 (2007) 37515–37528, https://doi.org/10.1074/jbc.M706399200.
[86] F. Marcelo, S. Huecas, L.B. Ruiz-Ávila, F.J. Cañada, A. Perona, A. Poveda, S. Martín-Santamaría, A. Morreale, J. Jiménez-Barbero, J.M. Andreu, J. Am. Chem. Soc. 135 (2013) 16418–16428, https://doi.org/10.1021/ja405515r.
[87] D.N. Margalit, L. Romberg, R.B. Mets, A.M. Hebert, J. Timothy, T.J. Mitchison, M.W. Kirschner, D.R. Chaudhuri, PNAS 101 (32) (2004) 11821–11826, https://doi.org/10.1073/pnas.0404439101.
[88] L.G. Czaplewski, I. Collins, E.A. Boyd, D. Brown, S.P. East, M. Gardiner, R. Fletcher, D.J. Haydon, V. Henstock, P. Ingram, C. Jones, C. Noula, L. Kennison, C. Rockley, V. Rose, H.B. Thomaides-Brears, R. Ure, M. Whittaker, N.R. Stokes, Bioorg. Med. Chem. Lett. 19 (2009) 524–527, https://doi.org/10.1016/j.bmcl.2008.11.021.
[89] A.L. Hopkins, C.R. Groom, A. Alex, Drug Discov. Today 9 (10) (2004) 430–431, https://doi.org/10.1016/S1359-6446(04)03069-7.
[90] J.M. Andreu, C. Schaffner-Barbero, S. Huecas, D. Alonso, M.L. Lopez-Rodriguez, L.B. Ruiz-Avila, R. Núñ EZ-Ramírez, O. Llorca, J. Martín-Galiano, J. Biol. Chem. 285 (19) (2010) 14239–14246, https://doi.org/10.1074/jbc.M109.094722.
[91] D.J. Haydon, N.R. Stokes, R. Ure, G. Galbraith, J.M. Bennett, D.R. Brown, P.J. Baker, V.V. Barynin, D.W. Rice, S.E. Sedelnikova, J.R. Heal, J.M. Sheridan, S.T. Aiwale, P.K. Chauhan, A. Srivastava, A. Taneja, I. Collins, J. Errington, L.G. Czaplewski, Science 321 (2008) 1673–1675, https://doi.org/10.1126/science.1159961.
[92] D.W. Adams, L.J. Wu, L.G. Czaplewski, J. Errington, Mol. Microbiol. 80 (1) (2011) 68–84, https://doi.org/10.1111/j.1365-2958.2011.07559.x.
[93] N.R. Stokes, N. Baker, J.M. Bennett, J. Berry, I. Collins, L.K. Czaplewski, A. Logan, R. Macdonald, L. Macleod, H. Peasley, J.P. Mitchell, N. Nayal, A. Yadav, A. Srivastava, D. Haydon, J. Antimicrob. Agents Chemother. 57 (1) (2013) 317–325, https://doi.org/10.1128/AAC.01580-12.
[94] T. Matsui, J. Yamane, N. Mogi, H. Yamaguchi, H. Takemoto, M. Yao, I. Tanaka, Acta Crystall. Sect. D 68 (2012) 1175–1188, https://doi.org/10.1107/S0907444912022640.
[95] N.L. Elsen, J. Lu, G. Parthasarathy, J.C. Reid, S. Sharma, S.M. Soisson, K.J. Lumb, J. Am. Chem. Soc. 134 (30) (2012) 12342–12345, https://doi.org/10.1021/ja303564a.
[96] S. Maa, C. Cong, X. Meng, S. Cao, H. Yang, Y. Guo, X. Lu, S. Maa, Bioorg. Med. Chem. Lett. 23 (2013) 4076–4079, https://doi.org/10.1016/j.bmcl.2013.05.056.
[97] M. Kaul, L. Mark, Y. Zhang, A.K. Parhi, Edmond J. LaVoie, D.S. Pilch, Antimicrob. Agents Chemother. 57 (12) (2013) 5860–5869, https://doi.org/10.1128/AAC.01016-13.
[98] M. Kaul, L. Mark, Y. Zhang, A.K. Parhi, Y.L. Lyu, J. Joan Pawlak, S. Saravolatz, L.D. Saravolatz, M.P. Weinstein, Edmond J. LaVoie, D.S. Pilch, Antimicrob. Agents Chemother. 59 (8) (2015) 4845–4855, https://doi.org/10.1128/AAC.00708-15.
[99] Alexander J. Lepak, A. Parhi, M. Madison, Karen Marchillo, Jamie Van Hecker, D.R. Andes, Antimicrob. Agents Chemother. 59 (10) (2015) 6568–6574, https://doi.org/10.1128/AAC.01464-15.
[100] M. Kaul, L. Mark, A.K. Parhi, E.J. LaVoie, D.S. Pilch, Antimicrob. Agents Chemother. 60 (2016) 4290–4296, https://doi.org/10.1128/AAC.00613-16.
[101] E.L. White, W.J. Suling, L.J. Ross, L.E. Seitz, R.C. Reynolds, J. Antimicro Chemother. 50 (2002) 111–114, https://doi.org/10.1093/jac/dkf075.
[102] R.C. Reynolds, S. Srivastava, L.J. Ross, W. Suling, E.L. White, Bioorg. Med. Chem. Lett. 14 (2004) 3161–3164, https://doi.org/10.1016/j.ejmech.2015.03.026.
[103] T.K. Beuria, M.K. Santra, D. Panda, Biochemistry 44 (2005) 16584–16593 PubMed: 16342949.
[104] C. Kelleya, S. Lu, A. Parhib, M. Kaul, D.S. Pilchc, E.J. LaVoiea, Eur. J. Med. Chem. 60 (2013) 395–409, https://doi.org/10.1016/j.ejmech.2012.12.027.
[105] B. Mathew, J.V. Hobrath, L. Ross, M.C. Connelly, H. Lofton, M. Rajagopalan, R.K. Guy, C. Robert, R.C. Reynolds, Plos One (2016) 1–23, https://doi.org/10.1371/journal.pone.0164100.
[106] J. Sun, M.H. Li, X.Y. Wang, Y. Zhang, R.J. Yuan, H.Y. Liu, H.L. Zhu, Vanillin derivatives as the selective small molecule inhibitors of FtsZ, Medl. Chem. Res. 23 (2014) 2985–2994, https://doi.org/10.1007/s00044-013-0886-8.
[107] A. Parhi, S. Lu, C. Kelley, M. Kaul, D.S. Pilch, E.J. LaVoie, Bioorg. Med. Chem. Lett. 22 (22) (2012) 6962–6966, https://doi.org/10.1016/j.bmcl.2012.08.123.
[108] C. Kelley, Y. Zhang, A. Parhi, M. Kaul, D.S. Pilch, E.J. LaVoie, Bioorg. Med. Chem. 20 (24) (2012) 7012–7029, https://doi.org/10.1016/j.bmc.2012.10.009.
[109] E. Nova, F. Montecinos, J.E. Brunet, R. Lagos, O. Monasterio, Biochem. Biophys. 465 (2) (2007) 315–319, https://doi.org/10.1016/j.abb.2007.06.032.
[110] T.K. Beuria, P. Singh, A. Surolia, D. Panda, Biochem. J. 423 (1) (2009) 61–69, https://doi.org/10.1042/BJ20090817.
[111] D. Dasgupta, Biochem. J. 423 (1) (2009) e1–e3, https://doi.org/10.1042/BJ20091226.
[112] K. Kumar, D. Awasthi, S.Y. Lee, I. Zanardi, B. Ruzsicska, S. Knudson, P.J. Tonge, R.A. Slayden, I. Ojima, J. Med. Chem. 54 (3) (2011) 74–381, https://doi.org/10.1021/jm1012006.
[113] L. Collins, S.G. Franzblau, Antimicrob. Agents Chemother. 41 (5) (1997) 1004–1009, https://doi.org/10.1128/AAC.41.5.1004.
[114] D. Awasthi, K. Kumar, S.E. Knudson, R.A. Slayden, I. Ojima, J. Med. Chem. 56 (2013) 9756–9770, https://doi.org/10.1021/jm401468w.
[115] S.E. Knudson, D. Awasthi, K. Kumar, A. Carreau, L. Goullieux, PLoS ONE 9 (4) (2014) e93953, https://doi.org/10.1371/journal.pone.0093953.
[116] B. Parka, D. Awasthia, S.R. Chowdhury, E.H. Melief, K. Kunal Kumar,

S.E. Knudson, R.A. Slayden, I. Ojima, Bioorg. Med. Chem. 22 (9) (2014) 2602–2612, https://doi.org/10.1016/j.bmc.2014.03.035.
[117] L.B. Ruiz-Avila, S. Huecas, M. Artola, A. Vergonos, E. Ramirez-Aportela, E. Cercenado, I. Barasoain, H. Vazquez-Villa, M. Martin-Fontecha, P. Chacon, M.L. Lopez-Rodriguez, J.M. Andreu, ACS Chem. Biol. 8 (2013) 2072–2083.
[118] M. Artola, L.B. Ruiz-Avila, A. Vergoñós, S. Huecas, L. Araujo-Bazán, M. Martín-Fontecha, M.L. López-Rodríguez, ACS Chem. Biol. 10 (3) (2014) 834–843, https://doi.org/10.1021/cb500974d.
[119] Q. Huang, F. Kirikae, T. Kirikae, A. Pepe, A. Amin, L. Respicio, I. Ojima, J. Med. Chem. 49 (2) (2006) 463–466, https://doi.org/10.1021/jm050920y.
[120] D. Singh, A. Anusri Bhattacharya, A. Ankit Rai, H. Pal, D. Singh, D. Divya Awasthi, I. Ojima, D. Panda, Biochemistry 53 (2014) 2979–2992, https://doi.org/10.1021/bi401356y.
[121] A.A. Handler, J.E. Lim, R. Losick, Peptideinhibitorofcytokinesis during sporulationin *Bacillus subtilis*, Mol. Microbiol. 68 (2008) 588–599, https://doi.org/10.1111/j.1365-2958.2008.06173.x.
[122] P. Bergman, L. Johansson, H. Wan, A. Jones, R.L. Gallo, G.H. Gudmundsson, T. Hökfelt, A.B. Jonsson, B. Agerberth, Infect. Immun. 74 (2006) 6982–6991 PubMed: 17030578.
[123] K.W. Shimotohno, F. Kawamura, Y. Natori, H. Nanamiya, J. Magae, H. Ogata, T. Endo, T. Suzuki, H. Yamaki, Biol. Pharm. Bull. 33 (4) (2010) 568–571 PubMed: 20410587.
[124] P. Paulasova, F. Pellestor, Ann. Genet. 47 (4) (2004) 349–358, https://doi.org/10.1016/j.anngen.2004.07.001.
[125] H. Gruegelsiepe, O. Brandt, R.K. Hartmann, J. Biol. Chem. 281 (41) (2006) 30613–30620, https://doi.org/10.1074/jbc.M603346200.
[126] J. Meng, F. Da, X. Ma, N. Wang, Y. Wang, H. Zhan, M. Li, Y. Zho, X. Xue, Z. Hou, M. Jia, X. Luo, Antimicrob. Agents Chemother. 59 (2014) 914–922, https://doi.org/10.1128/AAC.03781-14.
[127] J. Fujita, Y. Maeda, E. Mizohata, T. Inoue, M. Kaul, A.K. Parhi, E.J. LaVoie, D.S. Pilch, H. Matsumura, ACS Chem. Biol. 12 (2017) 1947–1955.